Heliyon 11 (2025) e42459

Contents lists available at ScienceDirect

Heliyon

journal homepage: www.cell.com/heliyon

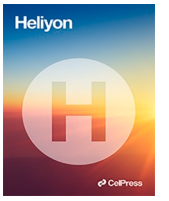

Research article

Analysis of changes in temperature and precipitation in South American countries and ecoregions: Comparison between reference conditions and three representative concentration pathways for 2050

Jaris Veneros [a,b,*], Andrew J Hansen [a], Patrick Jantz [c], Dave Roberts [a], Elkin Noguera-Urbano [d], Ligia García [e,f]

[a] Department of Ecology, Montana State University, Bozeman, MT, USA
[b] Facultad de Ingeniería y Ciencias Agrarias, Universidad Nacional Toribio Rodríguez de Mendoza de Amazonas, Chachapoyas, Amazonas, Peru
[c] School of Informatics, Computing and Cyber Systems, Northern Arizona University, Flagstaff, AZ, USA
[d] Alexander von Humboldt Biological Resources Research Institute, Bogotá, Colombia
[e] Instituto de Investigación para el Desarrollo Sustentable de Ceja de Selva (INDES-CES), Universidad Nacional Toribio Rodríguez de Mendoza de Amazonas, Chachapoyas, Amazonas, Peru
[f] Facultad de Ingeniería Zootecnista, Agronegocios y Biotecnología, Universidad Nacional Toribio Rodríguez de Mendoza de Amazonas, Chachapoyas, Amazonas, Peru

ARTICLE INFO

Keywords:
Sechura desert
Páramo
Napo moist forest
Climate change
Bioclim

ABSTRACT

Climate change is a global concern, and its impact on environmental variables such as temperature and annual precipitation is unknown spatially in the desert, andes, and rainforest ecoregions of Peru, Ecuador, and Colombia. In this study, we conducted a general review of climate drivers for South America (SA) and explored climate data using the GCM compareR package (General Circulation Models) and average ensembles for temperature and precipitation. Our results showed that all GCMs demonstrated increases in the annual mean temperature (BIO1) and in the mean temperature of the driest quarter (BIO9) for Peru, Ecuador, and Colombia for 2050 in three RCPs (2.6, 4.5, and 8.5). Also, most of the GCMs showed increases in the annual precipitation (BIO12) and the precipitation in the driest quarter (BIO17). We conducted non-parametric tests (Kruskal-Wallis Test) to assess if the medians of temperature and precipitation in the three ecoregions are equal for both the baseline and the climate change scenarios. We rejected the null hypothesis that the medians are equal for both temperatures and precipitation in the baseline vs. 2050 RCPs (2.6, 4.5, and 8.5). A spatial analysis was conducted to visualize the variations in temperature and precipitation between the RCPs versus the baseline, and the spatial variation at the country or ecoregion level can be observed. The annual mean temperature (°C) or annual precipitation (mm) divided by its standard deviation for each ecoregion (M metric) was analyzed to see how much the average temperature or the annual precipitation is relatively large compared to the variability or dispersion of temperatures or precipitation respectively; the average temperature and the annual precipitation for the baseline and the three RCPs are relatively large and associated with the variability or dispersion of their temperatures in the Napo moist forest compared to the other ecoregions. Our study provides important insights into the potential impacts of climate change on these ecosystems. Prospects in the Napo moist forest ecoregion, where

* Corresponding author.
E-mail address: jaris.veneros@untrm.edu.pe (J. Veneros).

https://doi.org/10.1016/j.heliyon.2025.e42459
Received 2 April 2024; Received in revised form 30 January 2025; Accepted 3 February 2025
Available online 5 February 2025

significant changes in temperature and humidity have already occurred, and new species have invaded or evolved in the western Amazon rainforest, are particularly highlighted and reflected in terms of risk mitigation, ecosystem restoration, surveillance, and monitoring.

1. Introduction

The Earth's climate has warmed, and precipitation regimes have changed over the last 100 years [1]. Alarming consequences of climate change on biodiversity have been suggested. It was mentioned that in the next century, many plants and animals will become extinct [2]. Climate change may have effects on different levels of Biodiversity, such as Genetics, Physiology, Phenology, Dynamics, Distribution, Interspecific Relationships, Community Productivity, Ecosystem Services, and Biome Integrity [3].

Latin America is home to a large concentration of plant and animal species and is estimated to be home to one-third of the world's terrestrial biodiversity [4]; it was also found that 43 % of all tree species on Earth are found in South America (SA) and that 40 % of the world's undiscovered tree species are found there [5].

The greatest risks of species extinction because of climate change are in South America, Australia, and New Zealand [6]. and the risks of species extinction due to climate change are not only expected to increase but to accelerate as global temperatures rise and changes in rainfall patterns [7]. Climate change is a statistically significant variation in the average state of the climate or its variability, which persists for a prolonged period (decades or more), and its origin may be due to internal natural processes or external factors, such as persistent changes in the atmosphere or land use [8,9]. These changes have been observed over the past 30 years, patterns of temperature, precipitation, humidity, and other environmental variables influencing flora, fauna, ecosystems, ecoregions, and biomes [9–11]. Research has reported the interaction of vegetation dynamics, sea surface temperature anomalies, and climate over time, making it important to understand these changes in the ecoregions of South America [12], and the use of remote sensing can complement temperature and precipitation data obtained from meteorological stations. For example, one study analyzed vegetation and climate dynamics in Italy between 2000 and 2021 using NDVI, LST, land cover, and precipitation data from MODIS [13]. Similarly, spatiotemporal changes in land surface temperature were analyzed in ecoregions of South Asia using MODIS data (2000–2021), revealing more intense diurnal cooling, nocturnal warming, and the influence of atmospheric oscillations [14].

Thus, in 1988, the Intergovernmental Panel on Climate Change (IPCC) was created to facilitate comprehensive assessments of climate change, its causes, potential impacts, and response strategies [15]. The first Assessment Report of the IPCC was completed in 1990. It provided the basis for the United Nations Framework Convention on Climate Change (UNFCCC), which included the 1990 IPCC Scenario A (SA90) and the 1992 IPCC Scenarios (IS92) were used in the Special Report on Emissions Scenarios (SRES) in 2000, in the Third Assessment Report (TAR) in 2001, and in the Fourth Assessment Report (AR4) in 2007 [16].

Then, the Fifth Assessment Report (AR5) on Climate Change was published between 2013 and 2014 where the IPCC chose to use scenarios developed by the scientific community, and four scenarios were elaborated, called Representative Concentration Pathways (RCPs), these represent different GHG emissions trajectories and are named according to the forced radiation they are expected to cause in the atmosphere in 2100 and are measured in $W/m^{2,}$ and these are RCPs 2.6. 4.5, 6.0, and 8.5 [17,18], and the lowest trajectory represents 2 °C above pre-industrial levels, and the highest trajectory is 8.5, which corresponds to a global warming of 4.5 °C or more above pre-industrial levels. In 2016, the first publications on Shared Socioeconomic Pathways (SSPs) were launched, and thanks to these, the IPCC's Sixth Assessment Report (AR6) on climate change was published in 2021 [19].

As computational systems have advanced, more regional or local analyses are now possible. For example, there are IPCC climate reference regions for subcontinental analysis of climate model data for South America, where they indicate that for RCP 8.5 (2081–2100), a temperature increase of greater than 4 °C is expected compared to 1986–2005 [11]. The proportion of extremely warm DJF days was observed to have at least doubled in recent decades in northern South America; less significant increases were observed in southern South America [20] Also, in future projections for 2010–2040 and 2070–2100, general warming is indicated throughout South America and in all its seasons, as well as more intense precipitation is estimated, but annual precipitation (mm) decreases, as well as delays in rainy seasons are expected throughout SA compared to the 1960–1990 baseline [21].

Warming is projected over South America and is of greater amplitude in the ETA Scenario forced by HadGEM2-ES RCP 8.5 (2011–2040, 2041–2070, and 2071–2100), warming begins in central and southeastern Brazil and progresses strongly toward the northern part of the SA and more intense precipitation is expected, but annual precipitation is decreasing compared to the 1961–1990 baseline [22].

Ideally, we should have monthly observed temperature and precipitation data for minimum periods of 30 years for Peru, Ecuador, and Colombia and with a resolution of greater than 1 km, but for now, we have annual meteorological data $\geq$ 1 km standardized for these areas, which can help us to understand the effects of the variation of these variables in ecoregions and/or vertebrate species for the areas under study. For instance, the spatiotemporal variability of precipitation and temperature trends (minimum, maximum, and average) was analyzed in 47 stations in the Brazilian Amazon for the period 1973–2013, the results showed that these had an increasing trend of approximately 0.04 °C per year and precipitation did not show a marked trend [23]. Other research helps to understand how oceanic conditions influence regional climate variability in Brazil. Extreme precipitation in the Brazilian Savanna, Pantanal, and Atlantic Forest presented no clear trend but suggested fewer intense rainfall days, while in the Amazon, Equatorial Pacific and Atlantic Sea Surface Temperature Anomalies (SSTAs) (Tropical North Atlantic Index - TNAI and Tropical South Atlantic Index - TSAI) correlated negatively with precipitation extremes and positively with air temperature [12].

In two climate change scenarios (RCPs 4.5 and 8.5), a reduction in precipitation of 2.4–11 % by 2050 and 2070, respectively, and an

increase in average annual temperature from 1.7 °C (HadGEM2-ES 2041–2060) and 3.7 °C (GFDL-CM3 2061–2080) in the Uribia-Guajira area compared to the baseline from 1976 to 2005 (IDEAM) are expected [24].

Evaluating climate data for Peru, Ecuador, and Colombia is difficult because of different interpolation methods, different periods for baselines, the selection of different global circulation models for climate change studies, and the lack of meteorological stations in their territories. The National Meteorological and Hydrological Services of Peru, Ecuador, and Colombia have few meteorological and hydrological stations in high-altitude areas as well as in Amazonian areas [25–27].

Also, analyzing minimum temperatures in the Andes is very complex in terms of error and uncertainty concerning maximum temperatures because of the altitude variation [27], and before using the SDMs, bioclimatic variables from different databases such as WorldClim must be analyzed. For example, variables derived from temperature and precipitation in our area of interest can provide preliminary information on the ecology of the species under study [28]. By having temperature (°C) and annual precipitation (mm) data, we could infer dry or rainy scenarios as well as analyze ensembles for different scenarios from published climate databases such as WorldClim, CHELSA, or CGIAR [29–32].

Within the NASA-sponsored Life on Land Project (2019–2023), one of the objectives was to review standardized climate data for a baseline and the year 2050 for Peru, Ecuador, and Colombia and generate information for the modeling of priority species to support its SDG 15. For this reason, we explored different databases for bioclimatic variables such as "ccafs" (Climate Change, Agriculture, and Food Security) with 10 min resolution and WorldClim (Global Climate Data) with 30 s resolution because they are standardized for the three countries [27,31]; in terms of Coordinate Reference Systems (CRS), resolution, and spatial extent.

A literature review and exploratory analysis of changes for two variables, temperature (°C) and annual precipitation (mm) for a baseline (1970–2000) and Climate Change Scenarios for 2050 (RCPs 2.6, 4.5, and 8.5) in three countries (Peru, Ecuador, and Colombia) and ecoregions (Sechura Desert, Páramos, and Napo Tropical Forest) were carried out. Then, statistical analyses of these environmental variables were conducted for these representative ecoregions: one from the Coast, one from the Andes, and one from the Tropical Rainforest. The purpose of this analysis was to investigate whether there is any significant difference between the means or medians of temperature and precipitation in the baseline and the 2050-RCPs (2.6, 4.5, and 8.5) within these ecoregions. The main contributions of this work are:

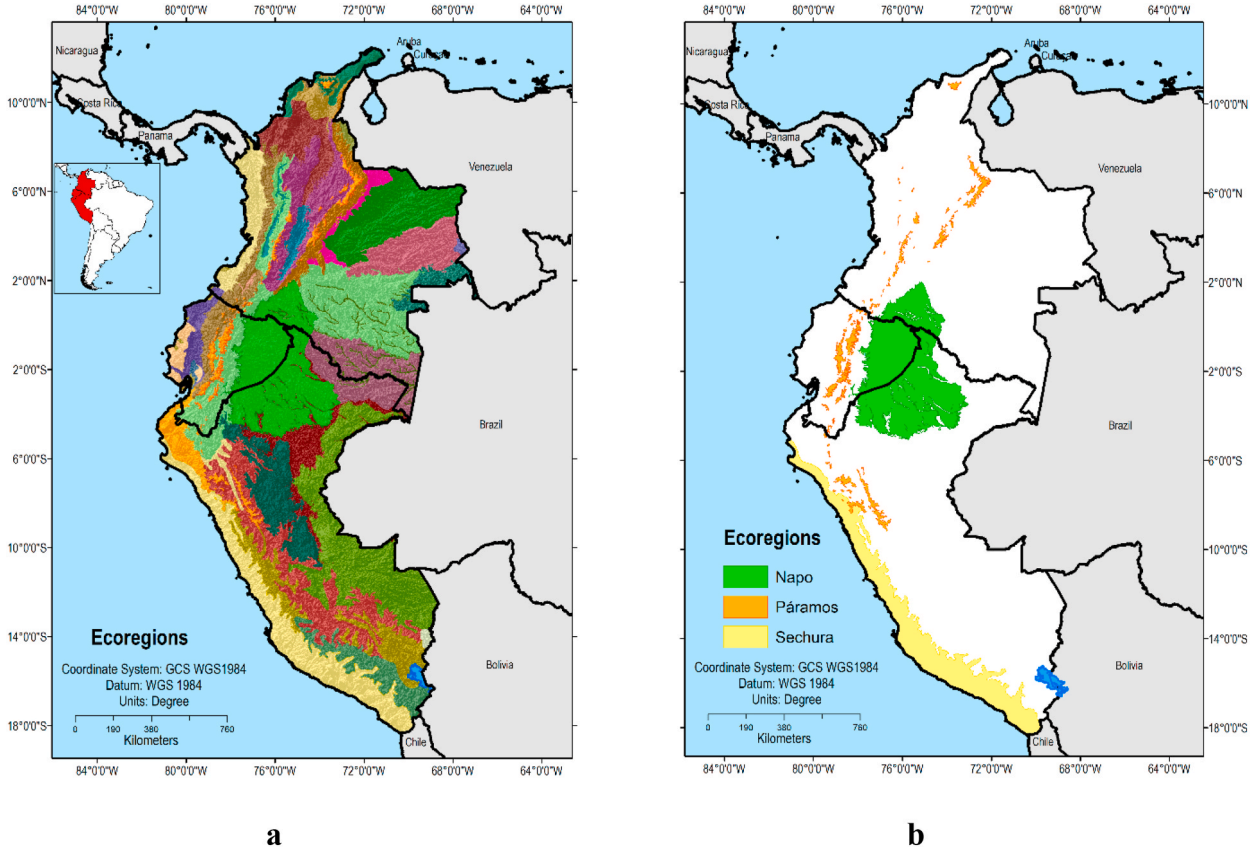

Fig. 1. a. Peru, Ecuador, and Colombia have 42 ecoregions b. Ecoregions under study Sechura Desert, Páramos, and Napo Tropical Forest ecoregions.

- Investigate how the annual mean temperature (°C) and annual precipitation (mm) will change between a baseline and the three RCP scenarios (2.6, 4.5, and 8.5) in 2050 in these three countries and ecoregions.
- Provide insights into the potential impact of climate change on these regions.

2. Methods

2.1. Study area

In this research, an analysis of climate change at the level of three countries, Peru, Ecuador, and Colombia (Fig. 1a), and in three ecoregions, Sechura Desert, Páramo, and Napo Tropical Forest (Fig. 1b) will be carried out. The Peruvian territory is located between the coordinates 0° and 18° 20′ of South Latitude and 68° 30′ and 81° 25' of West Longitude, covering an area of 1,285,215 km^2. Much of the territory comprises the Andes Mountains, which extend from South to North along the South American Continent. The Cordillera de Los Andes determines different geomorphological units typical of a continental environment and a marine environment [33].

Then, Ecuador is Located on the west coast and straddles the equator. Ecuador has a total area of about 280,000 km^2. Ecuador has a wide range of natural formations and climates, from the desert-like southern coast to the snowcapped peaks of the Andes Mountains to the plains of the Amazon River Basin. After that, Ecuador is bounded on the west by the Pacific Ocean, on the north by Colombia, and the east and south by Peru [34].

Lastly, Colombia is located between latitudes 12° 24′ north and 4° 17′ south and longitudes 66° 7′ and 79° west, and it has an area of 1,141,748 km^2. Colombia's topography has four general elements: the Andes Mountain system, which is united in a single knot at the border with Ecuador and then divides into three major mountain ranges that extend in a north-south direction and are known as the Cordillera Oriental, the Cordillera Central, and the Cordillera Occidental. The group of high mountains in the northeast of the country, between the Guajira peninsula and the Magdalena River valley, is known as the Sierra Nevada. The Bogotá Sabana is in the central-eastern part of the country, on the western side of the Eastern Cordillera. Finally, the great plains in the country's southeastern part extend from the Eastern Cordillera to the basins of the Orinoco and Amazon rivers in the east and southeast, this area is much larger than the mountainous and inhabited sector of the country. The great plains of the Orinoco and Amazon are uninhabited except for the tribes [35].

In addition, these countries have 47 ecoregions according to Resolve 2017, but for climate change studies, we used the Sechura Desert, Páramos like Santa Marta, Northern Andean, Cordillera Central and Cordillera de Mérida (Part of Venezuela) and Napo Tropical Forest ecoregions. The three ecoregions under study are described below (Fig. 1a and b) [36,37].

The Sechura Desert is in the western subtropical part of South America, bordering the Pacific Ocean to the west and extending between 20 and 100 km towards the Andean zone, and it is characterized by open shrub and tree stands [38,39]. The climate of the ecoregion is warm in summer and humid in winter, with average annual temperatures of 22 °C [39]. Precipitation in this ecoregion varies with altitude, from 0 mm/year to 250 mm/year, and this ecoregion is characterized by little vegetation cover, but it can be affected by the El Niño phenomenon [38–41].

The Páramo has the richest high mountain flora in the world and has a high degree of endemism [42]; for example, this region is home to the spectacled bear and the Andean tapir, both of which are endangered. The descriptions for the types of páramos used in this research are shown below.

First, the páramos of Santa Marta are the northernmost occurrence of this type of habitat in South America and are in the Sierra Nevada de Santa Marta, an isolated mountain massif that breaks away from the Andes and rises to 5775 m.a.s.l along the shores of the Caribbean Ocean in northern Colombia. The climate is influenced by northeasterly trade winds and rising humid air currents. Most of the rainfall occurs from May to September, with an estimated rainfall of less than 1800 mm/year; the average annual temperature is 6 °C. The northern part is more rugged and receives more precipitation than the southern part.

Second, the Northern Andean Páramo has a temperature range that goes from below freezing to 30 °C, the upper zone of the ecoregion receives more than 2000 mm/year of precipitation, and it has an average humidity of 80 % because it is in the Intertropical Convergence Zone (ITCZ), this slows tree growth and gives way to a tropical alpine grassland environment.

Third, the Cordillera Central Páramo extends in the vicinity of the Marañón Valley, from the extreme south of Ecuador to the northwest of Peru, and ranges in altitude from 3200 m to about 4500 m. The climate is cold and humid, and temperatures can drop below 0 °C. The typical landscape is that of treeless vegetation dominated by grass, and the shrubby alpine grassland is surrounded by montane cloud forest like the *Polylepis* transition forest.

In the end, the Cordillera de Merida Páramo's altitude ranges from 3000 m to approximately 4000 m, and these mountains are the highest peaks of the Andes in northwestern Venezuela. Precipitation ranges between 500 and 1000 mm/year, and in the dry season (December–March), less than 80 mm is accumulated. Snowfall is frequent in the highlands, especially during the wet season, although accumulation is unusual. The mean annual temperature at 4000 m is 2.8 °C with a daily fluctuation of 6 °C. At lower altitudes, daytime temperatures reach 21 °C but can drop to 0 °C at night.

In the Napo Moist Forests, its topography varies between lowlands and undulating also, it has swampy lands by the river systems [43]. The climate is humid and tropical, with a subtle dry season. The average annual temperature is 26 °C and can range from 12 to 38 °C. This ecoregion receives the highest annual rainfall in the Amazon, with up to 4000 mm in the west and 2500–3000 mm in the east. Three main vegetation types occur in this rainforest ecoregion: terra firme forest, várzea forest, and igapó swamp forest, but they are tall, evergreen tropical rainforests. These forests are among the richest in biodiversity of species in the entire Amazon basin and are among the most diverse in the world, with 219 species of mammals and 649 bird species recorded. This ecoregion is also an evolutionary and dispersal center for neotropical butterflies with high endemism.

2.2. Summary of the GCMs for climate change

The R package called GCM compareR and "ccafs" were used [27,29,] to access the Global Circulation Models (GCMs) of the Coupled Model Intercomparison Project Phase 5 (CMIP5) for the RCPs 2.6, 4.5, and 8.5 - 2050 [29]. Also, different climate change studies were analyzed for the three countries, especially changes in temperature (°C) and annual precipitation (mm) for different climate change scenarios up to 2050, as well as their effects on ecoregions. From some research, temperature and precipitation maps for climate change RCP scenarios for 2050 were rebuilt using ArcGIS ver. 10.7 georeferencing tools in the three countries [44]. In this way, more detailed climate information was extracted based on their coordinate system, and an overlay of our study areas with the rebuilt maps was then performed to have a clearer spatial interpretation.

2.3. Exploratory analysis for temperature and precipitation analysis

For the analysis of temperature (°C) and annual precipitation (mm) for 2050 under the RCP 2.6, 4.5, and 8.5 scenarios, 25 GCMs were used at the country level, and 26, 24, and 25 GCMs were used for ecoregions such as the Sechura Desert, Páramo, and Napo Moist Forest, respectively. The ensembles for the RCPs (2.6, 4.5, and 8.5) were made different GCMs for each RCP from the GCM Downscaled Data Portal of "ccafs: (CCAFS-CLIMATE) (http://ccafs-climate.org/data_spatial_downscaling/). Also, it should be noted that the number of GCMs varies depending on their availability for each country or ecoregion, and its resolution is 10 min ~ 18.5 km at the equator.

2.4. Statistical analysis: comparison medians at the ecoregion level

First, exploratory analyses of the temperature (°C) and annual precipitation (mm) medians were performed using the R package "ggridges" [45]. This package allows us to analyze the normality of temperature (°C) and annual precipitation (mm) in the three ecoregions under study.

The evaluation of the normal or non-normal distribution of the data for these variables for the baseline and RCPs allowed us to select the appropriate parametric and nonparametric tests for the comparison of means or medians, respectively [46]. The R package called "nor.test" was also used to analyze the normality analyses of the temperature and precipitation data for the baseline and the three climate change scenarios. The Anderson-Darling test, QQ plots, and histograms were used from this package [47].

The statistical analysis of medians comparisons for temperature (C°) and precipitation (mm) for the baseline (1970–2000) and the RCPs 2050 climate change scenarios ensembles (2.6, 4.5, and 8.5) was performed using the Kruskal-Wallis Nonparametric Test using the R Package 'palmerpenguins' in the software R-4.2.1 [48,49] in the Sechura Desert, Páramo, and Napo Moist Forest ecoregions.

The ensembles for the RCPs (2.6, 4.5, and 8.5) were made using 14 GCMs for each RCP from the WorldClim Database (https://www.WorldClim.org/data/v1.4/cmip5_30s.html) with a resolution of 30 s ~ 1 km at the equator. These GCMs were BCC-CSM1-1, CCSM4, CNRM-CM5, GFDL-CM3, GISS-E2-R, HadGEM2-AO, HadGEM2-ES, IPSL-CM5A-LR, MIROC5, MIROC-ESM, MIROC-ESM-CHEM, MRI-CGCM3, MPI-ESM-LR and NorESM1-M (For their names and origin, see Table S2). The Kruskal-Wallis is a nonparametric statistical test that assesses the differences among three or more independently sampled groups on a single, non-normally distributed continuous variable for non-normally distributed data [50,51].

3. Results

3.1. Drivers of Climate in South America

To comprehend the climate, we must define meteorology and climatology. Meteorology is the study of the atmosphere and the phenomena within it on scales ranging from minutes to weeks, and it focuses on atmospheric variables; otherwise, Climatology is the study of climates or long-term average atmospheric conditions over a place [52,53].

The weather is essentially the behavior of the atmosphere during the present time [,52,54]. The variables to characterize the weather for a particular place and time are usually temperature, precipitation, relative humidity (RH), cloud cover, wind speed, wind direction, and atmospheric pressure, and climate is the state of the atmosphere based on the record of observation and internationally accepted 30-year averages or climate in a wider sense is the state, including a statistical description, of the climate system [9,52,55].

Also, the climate of South America is very complex beyond the elements and factors of climate. The Andes Mountain range is the longest in the world [56–58] and extends from 11°N to 53°S. This mountain range crosses seven countries and is characterized by a great variety of ecosystems, and they are related to the climatic contrast on its east and west sides, as well as throughout its latitudinal extent [57].

The Sechura Desert, or the Atacama-Sechura Desert, is one of the driest and oldest deserts on Earth [41]. The formation of deserts such as the Sechura and Atacama (hyperarid) is due to these factors [41,59]: a. subtropical atmospheric subsidence; b. the Humboldt current, which runs from south to north and is cold, preventing precipitation in the coastal regions; and (3) the rain shadow effect of the Andes Mountains, which stops moist air from reaching the Pacific coast. A classification of aridity was made according to annual precipitation and is as follows: mesic $>$ 250 mm/y, semiarid $<$ 250 mm/y, arid $<$ 50 mm/y, and hyperarid $\leq$ 5 mm/y [41]. But we could not analyze the climate drivers of these deserts on their own because they are also due to the relationship they have with other ecoregions.

The hydroclimatic relationship between the Coast, Andes, and tropical forests has these factors [57]:

a) The atmospheric circulation in the Andes features a key trans-Andean flow at 5°S, influencing rainfall in northern Peru, Ecuador, and Colombia. During austral summer, the South American Monsoon System peaks, with the southern tropical Andes (8–27°S) blocking humid Amazon flows crucial for regional moisture. However, land use changes in the southeastern Amazon have reduced the flow's ability to regulate low flows.
b) The precipitation in the Andes is influenced by the ITCZ, westerly winds, Andean orography, local circulations, and temperature gradients. Low-Level Jets (LLJs) on both sides of the mountains, driven by flow blocking and mountain heating, play a key role in transporting moisture, except in subtropical regions west of the Andes.

Changes in atmospheric pressure or altitude cause changes in wind direction, and this also influences the climate of South America according to Ref. [57,60], additionally, moisture advection from the Amazon region is predominant during the austral summer. However, at latitudes of 5°S, where the altitude of the mountains is lower, trans-Andean flows are predominant throughout the year, producing a complex rainfall regime over this region. One of the rainiest places on Earth (Lloró; 5°30′N, 76°32′W) is located along the Pacific coast of Colombia, with an annual precipitation of 13,000 mm due to the dynamics of the low-level Chocó jet enhanced by atmosphere-ocean-land surface interactions [57,61,62].

3.2. Climate change review, exploration, and statistical analysis

General Circulation Models (GCMs) help to understand the impacts of climate change on our planet. This section presents two parts: the first is a review of the literature on the expected effects of climate change in our study areas, and the second is an exploratory review of GCMs at 10 min resolution and statistical analysis of temperature (°C) and annual precipitation (mm) for the RCPs 2.6, 4.5 and 8.5 for the Sechura Desert, Páramo, and Napo Moist Forest at 30 s resolution.

3.3. Climate change and its scenarios

In the history of our planet, it has been demonstrated that climate change could have natural as well as anthropogenic origins, so this research will analyze climate change events during the Anthropocene, using a baseline from 1970 to 2000, as well as its projections for the RCPs 2050 scenarios (Representative Concentration Pathways).

Climate change refers to a statistically significant variation in the mean state of the climate or in its variability that persists over an extended period, usually decades or longer [8]. Furthermore, climate change may be due to internal natural processes or external forcings or to persistent anthropogenic changes in the composition of the atmosphere or land use. Article 1 of the United Nations Framework Convention on Climate Change (UNFCCC) defines climate change as "a change of climate which is attributed directly or indirectly to human activity that changes the composition of the global atmosphere and which is in addition to natural climate variability observed over comparable periods" [8,63–65].

According to Ref. [66], the climate on our planet is a dynamic system, and in different millennia, we have had glacial periods and sea level changes caused mainly by the distribution of solar energy and atmospheric composition. In other ways, continental drift, mountain formation, and erosion have modified atmospheric and oceanic circulation patterns over longer time scales. Solar radiation has increased by 30 % over the last four billion years as the sun matured, but there are also predictable variations in the earth's orbit that influence the amount of solar radiation our planet receives at different times and latitudes, such as eccentricity, tilt, and precession. The periodicities of these orbital parameters are approximately 100,000, 41,000, and 23,000 years. The interactions between these Milankovitch cycles of solar input correlate with glacial and interglacial cycles. Analysis of these cycles indicates that the Earth would not naturally enter another ice age for at least 30,000 years, so natural cycles of solar input will not substantially compensate for human-induced climate warming.

The Anthropocene began around 1750 with the onset of the Industrial Revolution and is characterized by human domination of the biosphere [66]. Anthropogenic emissions of greenhouse gases have increased since the pre-industrial era, largely because of economic and population growth [66,67]. As a result, atmospheric concentrations of carbon dioxide, methane, and nitrous oxide have reached levels unparalleled in at least the last 800,000 years. The effects of emissions, as well as other anthropogenic factors, have been detected throughout the climate system and are likely to have been the dominant cause of the warming observed since the second half of the 20th century [68,69].

The estimated human contribution to global warming was estimated by the IPCC [68] for the period 1951–2010, the land temperature has increased by about 0.6 °C seen in the black bar whiskers with an uncertainty interval of 5 %–95 %, due to greenhouse gases or homogeneously mixed, other anthropogenic forcings (including the cooling effect of aerosols and the effect of land use changes), combined anthropogenic forcings, natural forcings, and natural internal variability (which is the element of climate variability that arises spontaneously in the climate system, even in the absence of forcings).

Climate scientists mentioned that global mean temperature and atmospheric carbon concentrations began to take on importance between the 1970s and 1980s, which gave climate change a global object to be studied on a global scale as well as its periodic assessments; thus, in 1990 the Intergovernmental Panel on Climate Change (IPCC) has been fundamental to the construction of a global ontology of climate change [70]. The IPCC was established by the World Meteorological Organization (WMO) and the United Nations Environment Programme (UNEP-UN) to assess scientific, technical, and socio-economic information for understanding the risk of human-induced climate change [68,71]. The 1994 IPCC assessment of the IS92 scenarios concluded that the scenarios were innovative and groundbreaking for that date, both regionally and globally; however, improvements should be made due to new global meteorological data, greenhouse gas data, as well as changing clean air policies adopted by some countries were having an effect [72]. The

IPCC has produced four generations of emissions scenarios [73]. Three were developed under its leadership: the 1990 Scientific Assessment (SA90), the 1992 IPCC Scenarios (IS92), and the Special Report on Emission Scenarios (SRES). The fourth comprises the Representative Concentration Pathways (RCPs) and the Shared Socioeconomic Pathways (SSPs), which served as the basis for Phases 5 and 6 of the Climate Model Intercomparison Project (CMIP5/CMIP6). The RCPs have been used in the scenario-based literature informing the IPCC Fifth Assessment Report (AR5), while the SSP/RCP combination will be used for the IPCC Sixth Assessment Report (AR6). CMIP6 selected the SSP/RCP combinations to be highlighted in AR6 [19].

On the other hand, as mentioned above, in this research, we will analyze and use the RCP scenarios in South America. The RCPs are a set of four pathways developed by the IPCC and published in 2014 (AR5), and they were developed based on the concentration trajectory of greenhouse gases in the atmosphere [68]. The four RCPs cover the range of radiative forcing values for the year 2100, and they are 2.6, 4.5, 6.0, and 8.5 W/m^2 [22,68,73].

For the development of the RCPs, seven steps were considered seven steps within three groups; for example: Integrated Assessment Models (IAMs), Processing and Completion, and RCP repository, where the RCPs are based on scenarios published in the existing literature in terms of emissions and concentrations, they provide information on all components of radiative forcing that are needed as input for climate and atmospheric chemistry modeling such as greenhouse gas emissions and land use, and this data was harmonized over the base year for emissions and land use for historical and future period analyses (2100) [74].

The RCPs should not be interpreted as forecasts or absolute limits, nor should they be viewed as prescriptive policies [74,75]. The RCPs describe a set of possible developments in emissions and land use based on consistent scenarios representative of the current literature [74]. The RCPs scenarios encompass a time series of emissions and concentrations of the full range of greenhouse gases and, aerosols and chemically active gases, as well as land use and land cover. The word "representative" means that each concentration trajectory provides one of many possible scenarios that would lead to specific radiative forcing characteristics. The word trajectory emphasizes that only long-term concentration levels are of interest but also indicates the path followed over time to arrive at the outcome in question [18,76]. Representative concentration trajectories generally refer to the part of the concentration trajectory up to the year 2100, for which models have been used to model the concentration trajectory 2100, for which the integrated assessment models have generated the corresponding emissions scenarios [68,74].

i. RCP 2.6: Trajectory in which radiative forcing peaks at about 3 W/m^2 before 2100 and then decreases (the corresponding extended concentration trajectory under the assumption of constant emissions after 2100).
ii. RCP 4.5 and RCP6.0: Two intermediate stabilization trajectories in which radiative forcing stabilizes at about 4.5 W/m^2 and 6.0 W/m^2 after 2100 (the corresponding extended concentration trajectory under the assumption that concentrations are constant after 2150).
iii. RCP 8.5: High trajectory for which radiative forcing reaches values $>$ 8.5 W/m^2 in 2100 and continues to increase for a time lag (the corresponding extended concentration trajectory assuming constant emissions after 2100 and constant concentrations after 2250).

3.4. *Climate change review in ecoregions*

In South America (SA), the effects of climate change on temperature and precipitation for 2050–2080 were analyzed with a baseline from 1980 to 2005; the results showed that for the austral summer (DJF) and winter (JJA), there will be an increase in the frequency and intensity of extreme daily rainfall events over the southeast and extreme north of South America; furthermore, in the Amazon during DJF, there is a statistically significant increase in the number of consecutive dry days and a decrease in the number of consecutive wet days [53]. In addition, deforestation, fires, and deaths associated with extreme weather conditions, such as droughts, have generated the Amazon forests to become savannah [77]; as a result, studies of climate change in this type of Biome are urgently needed.

Some dynamic vegetation models have been used, and the results of the projections show that some areas of tropical rainforest in the Amazon region are replaced by deciduous forests and grasslands in the RCP 4.5 scenario and only by grasslands in the RCP 8.5 scenario at the end of this century; however, a reduction of the Amazon biome can generate a positive feedback of the temperature increase and affect the regional hydrological cycle [78]. Also, warming is projected throughout South America, with greater amplitude in the Eta scenario forced by HadGEM2-ES RCP 8.5 based on the baseline period, 1961–1990, and three-time slices 2011–2040, 2041–2070, and 2071–2100, and for the two emission scenarios RCP 4.5 and RCP 8.5 and precipitation in DJF, there will be the greatest reduction from NO to CS regions, an area generally occupied by the South Atlantic Convergence Zone (SACZ) [22]. Other research related to the formation of savannas for future climates (RCP 8.5) in the Amazon and Northern Brazil where it is stated that there is a possible increase in the aridity of 33.8 % and 36.9 % (UNEP index) and 4.6 % and 13.9 % (Budyko index) respectively, by the end of the 21st century [79]. Otherwise, preserving the Amazon is of great importance for the hydrological cycle, for example, the fraction of the mean annual precipitation that has been transpired by trees in the Amazon basin can be as high as 50 % [57,80]. More studies are needed to understand the hydrological relationship between the Andes and the Amazon rainforest in the context of climate change.

In general, climate change studies and analyses of temperature and precipitation for the Sechura, Páramo, and Napo ecoregions are very scarce (Table S1), and studies are usually presented for all of South America.

In scenarios of climate change (2035–2065 RCP 8.5 - 1 km of resolution), the Sechura desert is expected in most of the zones; there will be no changes that will affect its biome, however, in some zones, there may be an increase in vertical structure as well as in humidity compared to 1981–2010 climate data (Table S1) [81]. Also, in the northern zone of the Sechura Desert by 2100 (26 GCMs

from CMIP5 in the four RCPs scenarios with a resolution of 1° × 1°), the temperature is expected to increase by over 1.5 °C and the annual precipitation from 50 to over 150 mm/year relative to the pre-industrial period (1861–1890) [82].

In Peru, Ecuador, Colombia, and Venezuela for the A1B 2010–2039 and A1B 2040–2069 scenarios, the páramo shows a loss of potential and remaining area concerning the year 2000 [83]. In potential areas, part of the páramo will be replaced by forest biomes, but the páramo appears to be more affected by land use change than by climate change. Projections suggest that the páramo shows an upward shift, and an average loss of 31.4 % is projected for the potential distribution but only 25 % for the remnant areas (A1B, 2010–2039) (Table S1) [83,84]. In this way, Páramos, located at the highest elevations, are the most at risk due to the lack of upland areas for migration [83]. Also, Páramos have soils with high organic matter content as well as high humidity, which conditions their presence [83,85].

Then, the Tropical forests are threatened by deforestation, fragmentation, land use change, and climate change in South America [86]. However, vegetation also regulates climate, so it was found that exposure to heat stress due to deforestation was comparable to the effect of climate change under RCP 8.5 (2073–2100) compared to a historical period (1980–2010) in the Napo ecoregion [87] and increases in its mean annual temperature and annual precipitation for 2030, 2050 and 2080; for example, the RCP 8.5 (5 km resolution) for 2080 shows an increase in average temperature for this ecoregion of 4.2 °C and 349 mm in annual precipitation compared to a 1981 to 2010 baseline (Table S1) [88].

3.5. Temperature and precipitation: exploratory and statistical analysis

For the analysis of temperature and precipitation for 2050 under the RCP 2.6, 4.5, and 8.5 scenarios, 25 GCMs were used at the country level, and 26, 24, and 25 GCMs (10 min of resolution) were used for ecoregions such as the Sechura Desert, Páramo, and Napo Moist Forest, respectively; it should be noted that the number of GCMs varies depending on their availability for each country or ecoregion. For details of the GCMs, such as the average temperature and precipitation values for the baseline and their names and origins, see these tables in the supplementary data (Tables S2, S3, S4, S5, S6).

Table 1 shows the changes in average annual temperatures (°C) for the three countries and three ecoregions. The second column shows annual average temperatures for the baseline (1970–2000) for these areas. The temperature variations for RCPs 2.6, 4.5, and 8.5 are shown below, where the minimum and maximum values of the differences between the mean temperatures of the set of GCMs for 2050 of the three RCPs relative to the baseline were selected. These differences in minimum values, maximum values, and ensembles all have positive signs, so it is expected that the annual mean temperature will increase in all study areas and all scenarios.

In addition, Table 2 below shows the changes in annual precipitation (mm) for the three countries and the three ecoregions. The second column shows the average annual precipitation from 1970 to 2000 for these zones. The annual precipitation changes for RCPs 2.6, 4.5, and 8.5 are shown below, where the differences between the annual precipitation of the 2050 RCPs with the baseline indicate that annual precipitation will increase (where the sign is positive) in all study zones and all scenarios; however, some GCMs have negative signs, which indicate that there is a reduction in the annual precipitation by 2050 in the three RCPs. Then, the GCMs indicating the greatest reduction in precipitation (negative sign), as well as the GCMs indicating the greatest increase in precipitation (positive sign), were selected for these RCPs. Finally, all ensembles for the three RCPs indicated that annual precipitation would increase by 2050.

The spatial variation of the differences of the 25 GCMs (10 min resolution) for the temperature (°C) vs. annual precipitation (mm) variables for the three countries for the three RCPs vs. the baseline are shown in Figs. 2–7. Figures S2.1, S2.2, and S2.3 show the annual precipitation (mm) versus temperature (°C) variables in the three countries for the three RCPs 2050. These figures help us to identify the GCMs with low annual precipitation and low temperature or high annual precipitation and high temperature or low annual precipitation and high temperature or high annual precipitation and low temperature, as well as their proximity to the ensembles. Also, the spatial variation of the differences of different GCMs (10 min resolution) for the Mean Temperature of Driest Quarter bio9 (°C) vs. Precipitation of Driest Quarter bio17 (mm) in the three countries for the three RCPs (2.6–26 GCMs, 4.5–31 GCMs and 8.5–32 GCMs) vs. the baseline are shown in Figs. 8–13.

All GCMs (26 GCMs RCP-2.6, 31 GCMs RCP-4.5, and 32 GCMs RCP-8.5) show temperature increases for the Mean Temperature of Driest Quarter bio9 (°C) when the difference between the RCPs-2050 minus the baseline was made. For example, the following shows how much temperatures will increase in the driest quarter for the three RCPs-2050 in the three countries in the driest quarter: 3.17 °C

Table 1
Average annual temperature (°C) differences for 2050 RCPs and baseline (1970–2000) (10 min) at the country and ecoregion level.

Countries and ecoregions	Baseline T °C	RCP2.6			RCP 4.5			RCP 8.5		
		Min value	Max value	Ensemble	Min value	Max value	Ensemble	Min value	Max value	Ensemble
Peru, Ecuador, and Colombia	21.7	1.0	2.8	1.6	1.0	3.4	1.9	1.5	4.2	2.7
Sechura Desert (Deserts & Xeric Shrublands)	15.0	1.0	2.4	1.6	0.9	3.0	1.9	2.1	3.7	2.7
Páramo (Montane Grasslands & Shrublands)	7.5	0.9	2.4	1.5	1.1	3.0	1.8	1.7	3.8	2.6
Napo moist forests (Tropical & Subtropical Moist Broadleaf Forests)	25.7	0.9	3.3	1.6	1.0	4.0	2.0	1.7	4.9	2.8

Table 2
Annual precipitation (mm) differences for 2050 RCPs and baseline (1970–2000) (10 min) at the country and ecoregion level.

Countries and ecoregions	Baseline mm	RCP2.6			RCP 4.5			RCP 8.5		
		Min value	Max value	Ensemble	Min value	Max value	Ensemble	Min value	Max value	Ensemble
Peru, Ecuador, and Colombia	2068.7	−117.5	144.9	48.5	−160.6	219.0	64.5	−210.4	279.2	71.4
Sechura Desert (Deserts & Xeric Shrublands)	190.3	−11.6	196.1	49.1	−13.2	237.3	64.3	−3.5	286.3	81.8
Páramo (Montane Grasslands & Shrublands)	1206.5	−98.8	241.0	73.9	−87.0	70.9	93.3	−50.2	165.2	96.2
Napo moist forests (Tropical & Subtropical Moist Broadleaf Forests)	2825.1	−233.7	195.3	5.0	−415.2	381.9	30.7	−487.7	472.7	40.5

(RCP-2.6), 3.95 °C (RCP-4.5) and 4.72 °C (RCP-8.5) compared to the baseline (Tables S4, S5, and S6). Otherwise, most of the GCMs for the three RCPs in 2050 for the three countries indicate that there is an increase in precipitation of Driest Quarter bio17 (mm) with maximum values of 26.66 mm (RCP-2.6), 47.47 mm (RCP 4.5) and 47.04 mm (RCP 8.5) (Tables S4, S5, and S6).

Four tables are shown below: two for temperature (°C) ensembles (Tables 3 and 4) and the others for precipitation (mm) (Tables 4 and 5) for the baseline and the 2050-RCPs in the three ecoregions (1 km resolution). These ensembles were constructed from 14 GCMs.

The minimum temperatures of the Sechura Desert are below zero degrees and are at a higher altitude. Likewise, their minimum temperatures remain below zero for all three RCPs in 2050 concerning the baseline. On the other hand, for maximum temperatures, there is an increase from 1.82 °C, 2.17 °C, and 2.55 °C for RCPs 2.6, 4.5, and 8.5 in 2050 concerning the baseline. Furthermore, the minimum temperatures in the Páramo decrease only for RCP 2.6 by 0.31 °C but not for RCPs 4.5 and 8.5 compared to the baseline. Otherwise, maximum temperatures increase from 1.21 °C to 1.93 °C in 2050 at the baseline. Average temperatures increase from 1.24 °C, 1.63 °C, and 2.11 °C for RCPs 2.6, 4.5, and 8.5 in 2050 from 1970 to 2000. Lastly, the minimum temperatures of the Napo increased for the three RCPs by 0.73 °C, 1.16 °C, and 1.65 °C compared to the baseline. Otherwise, maximum temperatures increase from 1.44 °C to 2.44 °C in 2050 compared to the baseline. Average temperatures increase from 1.59 °C, 2.02 °C, and 2.56 °C for RCPs 2.6, 4.5, and 8.5 in 2050 compared to 1970–2000.

The standard deviations for the temperature values for the baseline and the three climate change scenarios 2050 RCPs were also analyzed for each ecoregion, where the Sechura Desert has the highest deviations compared to the Páramo and Napo (Tables 3 and 4), possibly due to the large variation in altitude of this ecoregion.

The annual precipitation was also analyzed for the 1970–2000 and the three 2050 RCPs in the three ecoregions (Tables 5 and 6). The Sechura desert presented the lowest annual precipitation with 183.72 mm (minimum precipitation of 0 and maximum of 1194 mm). For the three climate change scenarios, there will also be zero precipitation values, but there will be an increase in the maximum annual precipitation compared to 1970–2000. The páramo has an annual precipitation of 1151.41 mm with a minimum of 262.00 mm and a maximum of 3169.00 mm for 1970–2000. The climate change scenarios for 2050-RCPs show increases in both the average annual precipitation and its minimum and maximum values concerning the baseline. Ultimately, Napo has an annual precipitation of 2977.45 mm with a minimum precipitation of 1630.00 mm and a maximum of 4778.00 mm. The annual precipitation for this ecoregion does not increase for the scenario 2.6, but it does for scenarios 4.5 and 8.5. On the other hand, the minimum and maximum precipitation for the three climate change scenarios increase, the maximum precipitation presents an increase of over 469.5 mm per year. On the other hand, the minimum and maximum precipitation for the three climate change scenarios (RCPs 2.6, 4.5, and 8.5) increased, the minimum precipitation presented an increase of over 210.21 mm, and the maximum precipitation presented an increase of over 469.5 mm per year.

The standard deviation for annual precipitation in the Sechura desert for 1970–2000 is 225.50 and the standard deviations for RCPs 2.6, 4.5, and 8.5 in 2050 are above this value. For the Páramo, the standard deviation is 329.50 in its baseline, and for the three RCPs, their standard deviations are above this value. Lastly, the standard deviation of the Napo for the baseline is 493.47, and this decreases for RCPs 2.6, 4.5, and 8.5 in 2050, and these are their values of 471.72, 476.07, and 479.75, respectively.

The spatial variation of the differences of the ensembles made for temperature (°C) and annual precipitation (mm) for RCPs 2.6, 4.5, and 8.5 by 2050 from the 14 GCMs vs. the baseline (1 km resolution) for the three ecoregions are shown in Figs. 14–16. For the Sechura desert in the three RCPs, temperatures with maximums of over 6.10 (°C) were observed for the central-southern part, while annual precipitation (mm) decreases for the coastal part but increases for the areas near the Andes Mountains. Also, in the Páramo ecoregion for the three RCPs, increases in mean annual temperature with maximums of over 10 (°C) were noted; in terms of precipitation, a decrease in annual precipitation is observed for the páramos of Peru, Ecuador, and Venezuela in most areas. In the Napo, there are pronounced temperature increases in the eastern part (maximum temperatures above 2.71 °C) and a decrease in temperature in the western part, and for annual precipitation, there is a decrease in the central part of this ecoregion and an increase in the northern and southwestern part.

Finally, the average temperature (°C) or annual precipitation (mm) divided by its standard deviation for each ecoregion (M metric) was analyzed to see how much the average temperature or the annual precipitation is relatively large compared to the variability or dispersion of temperatures or precipitation respectively (From Tables 3–6). For example, the temperature (°C) in the Napo moist forests obtained a higher value for the M metric in the baseline, and the three RCPs-2050 (2.6, 4.5, and 8.5) and these values were 34.19, 37.30, 35.92, and 36.15 respectively. Also, in this ecoregion, the precipitation (mm) obtained higher values for the M metric in

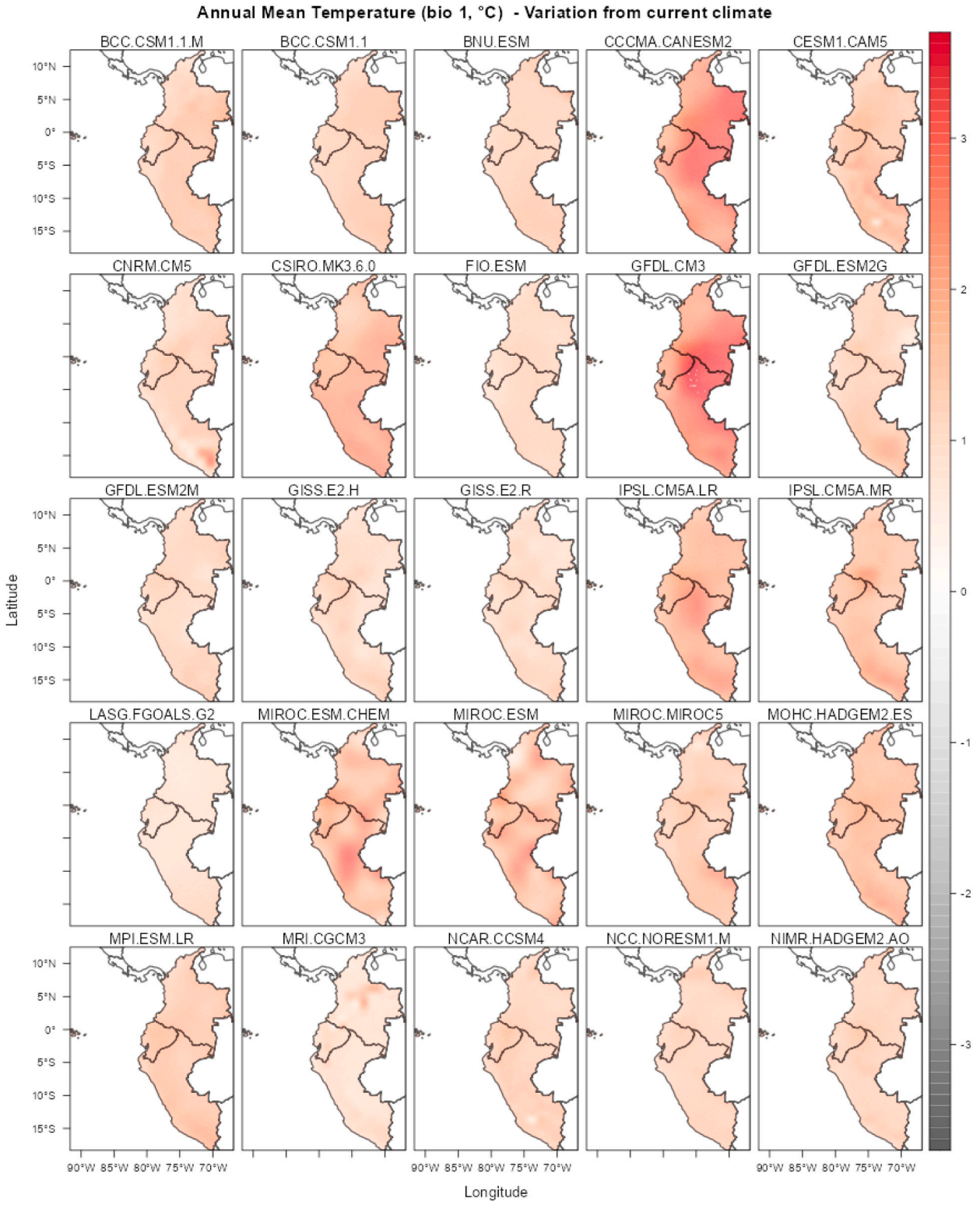

Fig. 2. Differences for temperature (°C) for the RCP 2.6-2050 and the baseline (1970–2000). Where red indicates an increase in temperature, while gray indicates a decrease.

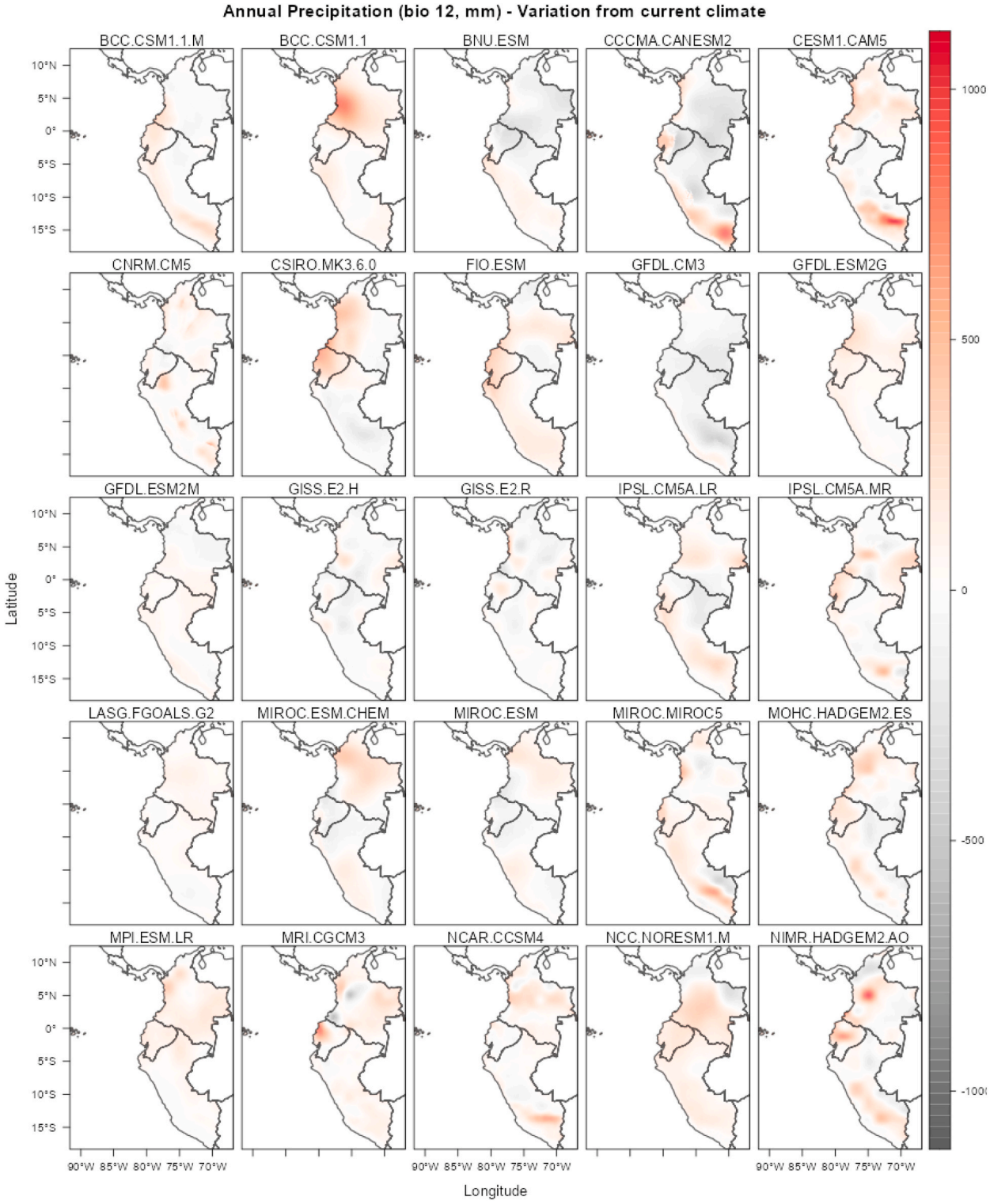

Fig. 3. Differences for annual precipitation (mm) for the RCP 2.6-2050 and the baseline (1970–2000). Where red indicates an increase in temperature, while gray indicates a decrease.

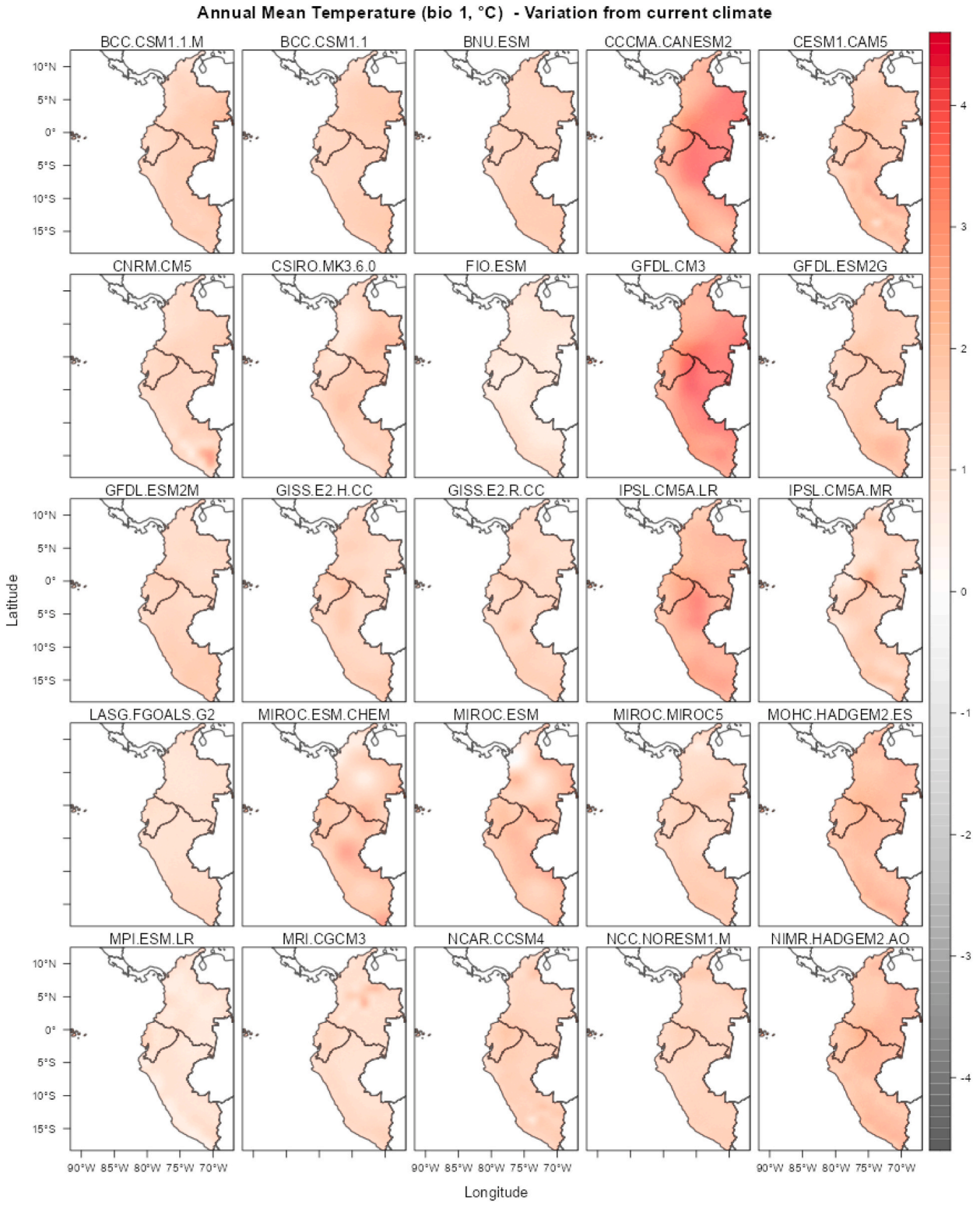

Fig. 4. Differences for temperature (°C) for the RCP 4.5-2050 and the baseline (1970–2000). Where red indicates an increase in temperature, while gray indicates a decrease.

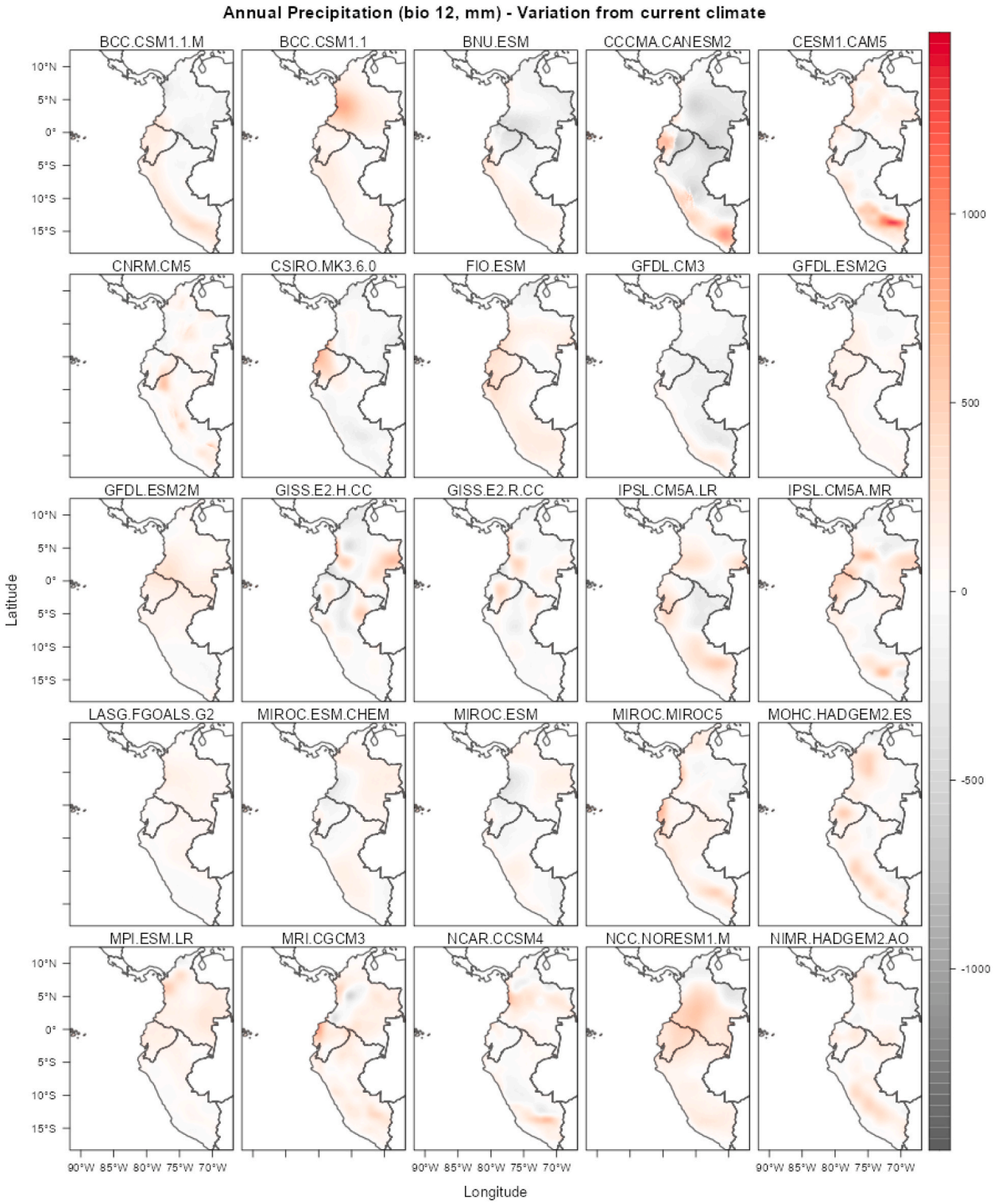

Fig. 5. Differences for annual precipitation (mm) for the RCP 4.5-2050 and the baseline (1970–2000). Where red indicates an increase in temperature, while gray indicates a decrease.

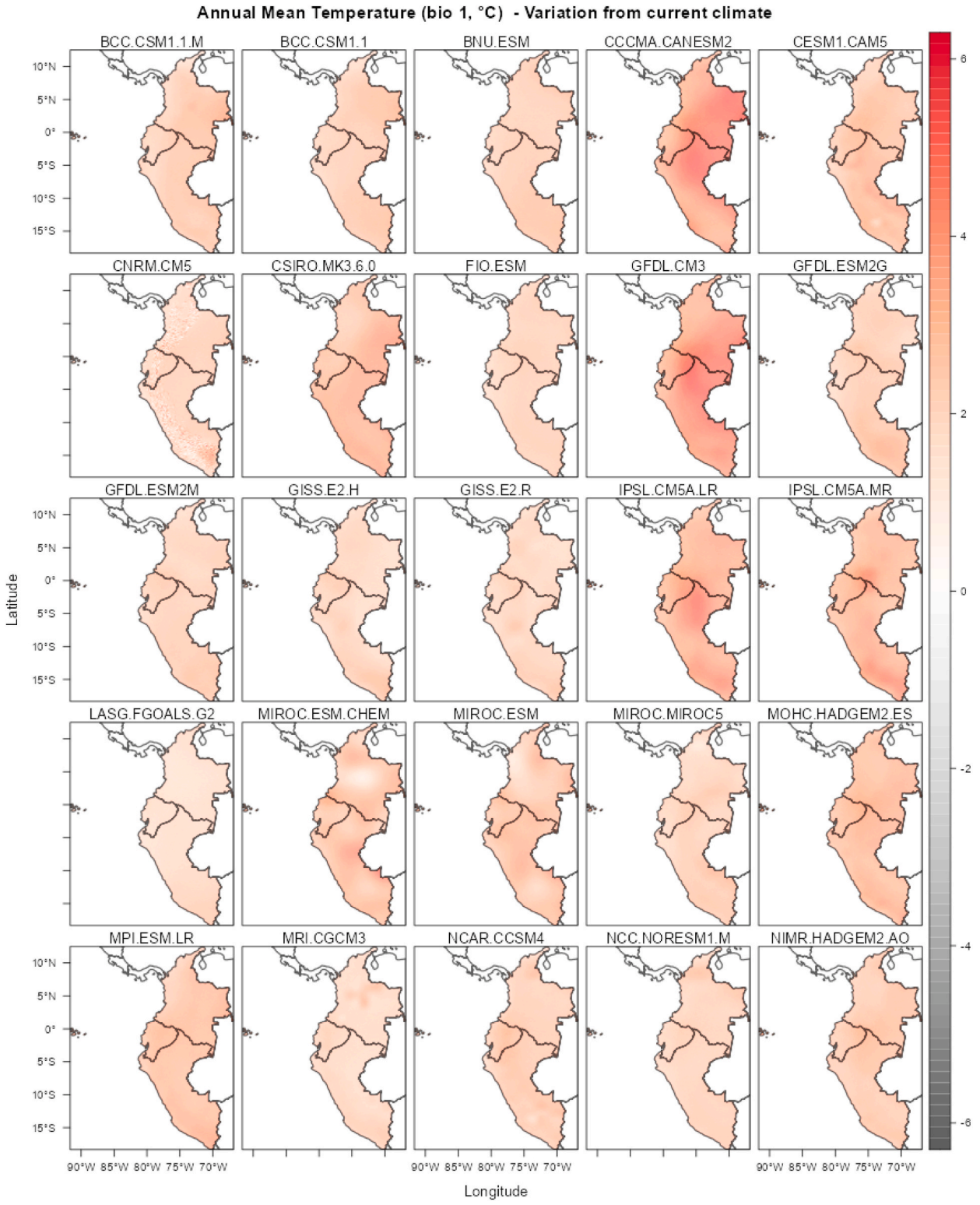

Fig. 6. Differences for temperature (°C) for the RCP 8.5-2050 and the baseline (1970–2000). Where red indicates an increase in temperature, while gray indicates a decrease.

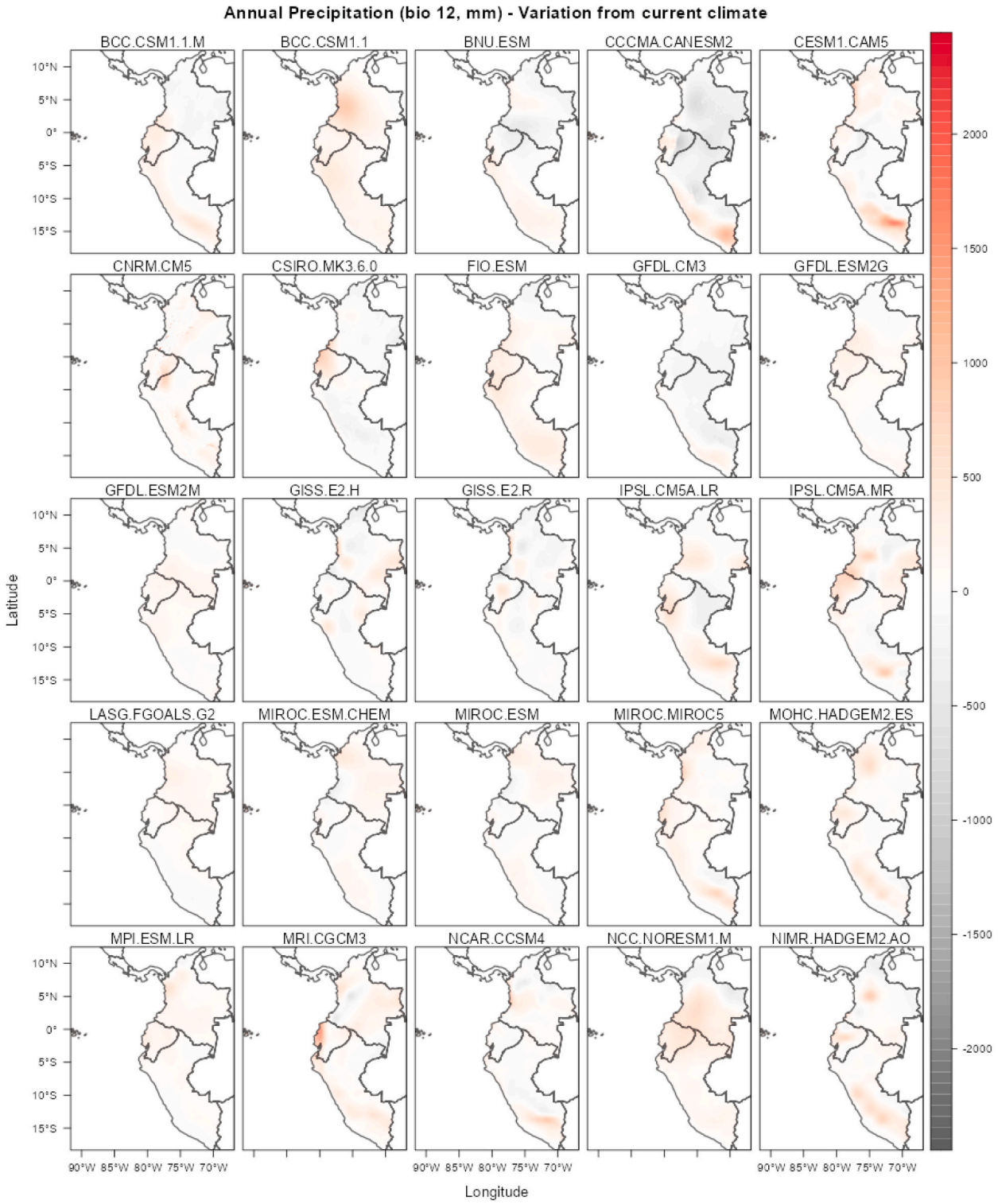

Fig. 7. Differences for annual precipitation (mm) for the RCP 8.5-2050 and the baseline (1970–2000). Where red indicates an increase in temperature, while gray indicates a decrease.

the baseline and the three RCPs-2050 (2.6, 4.5, and 8.5), and these values were 6.03, 6.05, 6.17 and 6.13 respectively, suggesting that the average temperature and the annual precipitation for the baseline and the three RCPs are relatively large associated to the variability or dispersion of their temperatures compared to the other two ecoregions such as Sechura Desert and Páramo.

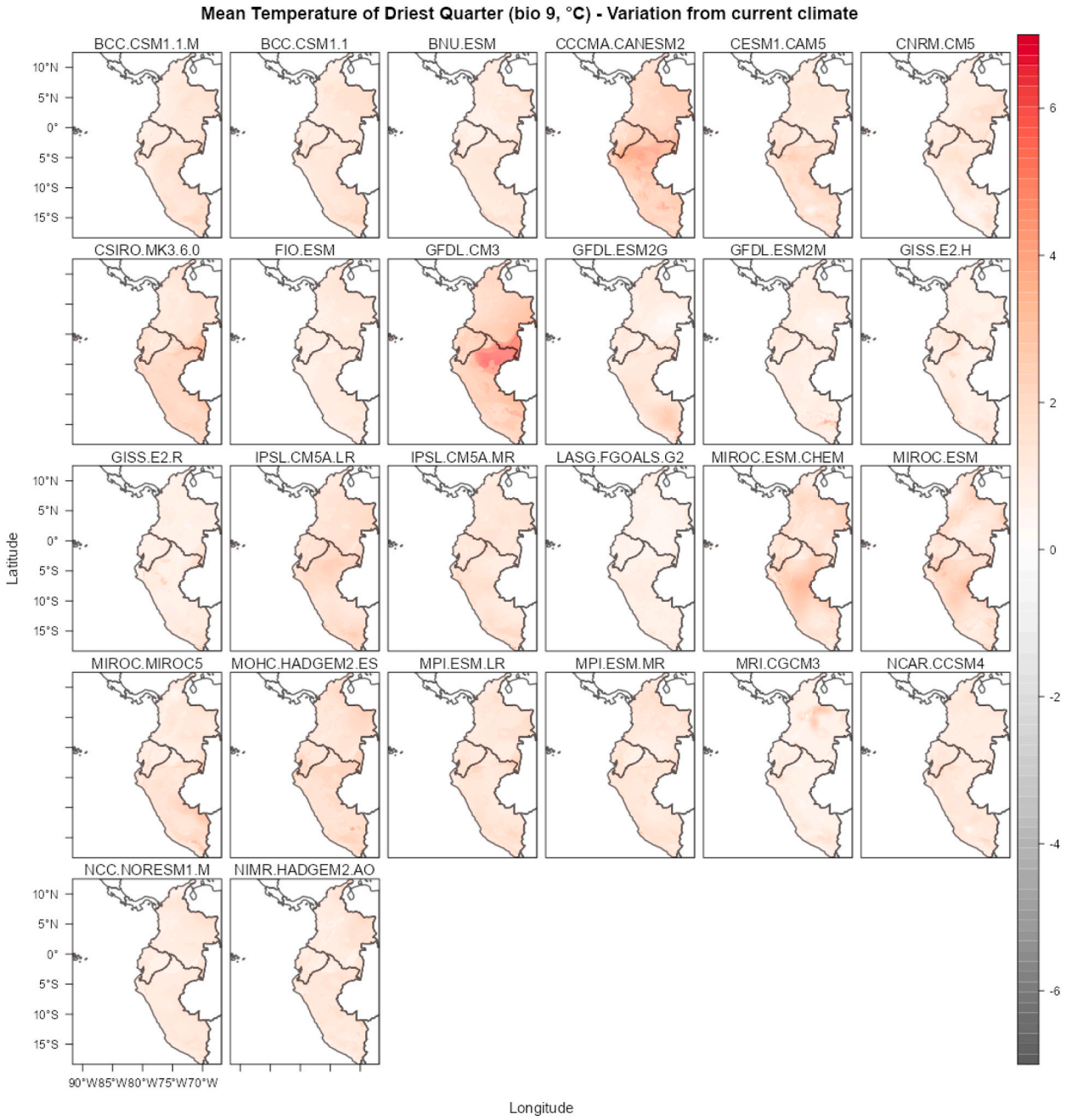

Fig. 8. Differences for the Mean Temperature of Driest Quarter bio9 (°C) for the RCP 2.6-2050 and the baseline (1970–2000). Where red indicates an increase in temperature, while gray indicates a decrease.

3.5.1. Sechura Ecoregion

The distribution of temperature (°C) and precipitation (mm) for 1970–2000 and three climate change scenarios for the Sechura (Desert) ecoregion, respectively, are shown in Figs. 17 and 18, showing the non-normal distribution of the data. In the case of temperature, there is a bimodal distribution (Fig. 17), and in the case of precipitation, there is a skewed right distribution (mean > median) (Fig. 18). Q-Q plots, histograms, and boxplots for temperature and precipitation for the baseline (1970–2000) and the three RCPs 2.6, 4.5, and 8.5 for 2050 in the Sechura ecoregion were analyzed and suggest that there are serious violations of normality assumptions (Skewed) and several atypical values for low temperatures and high precipitation (Figures S4, S5 and S6).

The Anderson-Darling normality test was performed for the temperature (°C) (Table S10) and precipitation data (mm) (Table S11) for this ecoregion; there is very strong evidence to reject the null hypothesis that the data follow a normal distribution for the baseline and the three RCPs in 2050. Therefore, the alternative hypothesis that temperature (*p-value* $= 3.7 \times 10^{-24}$) and precipitation (*p-value*

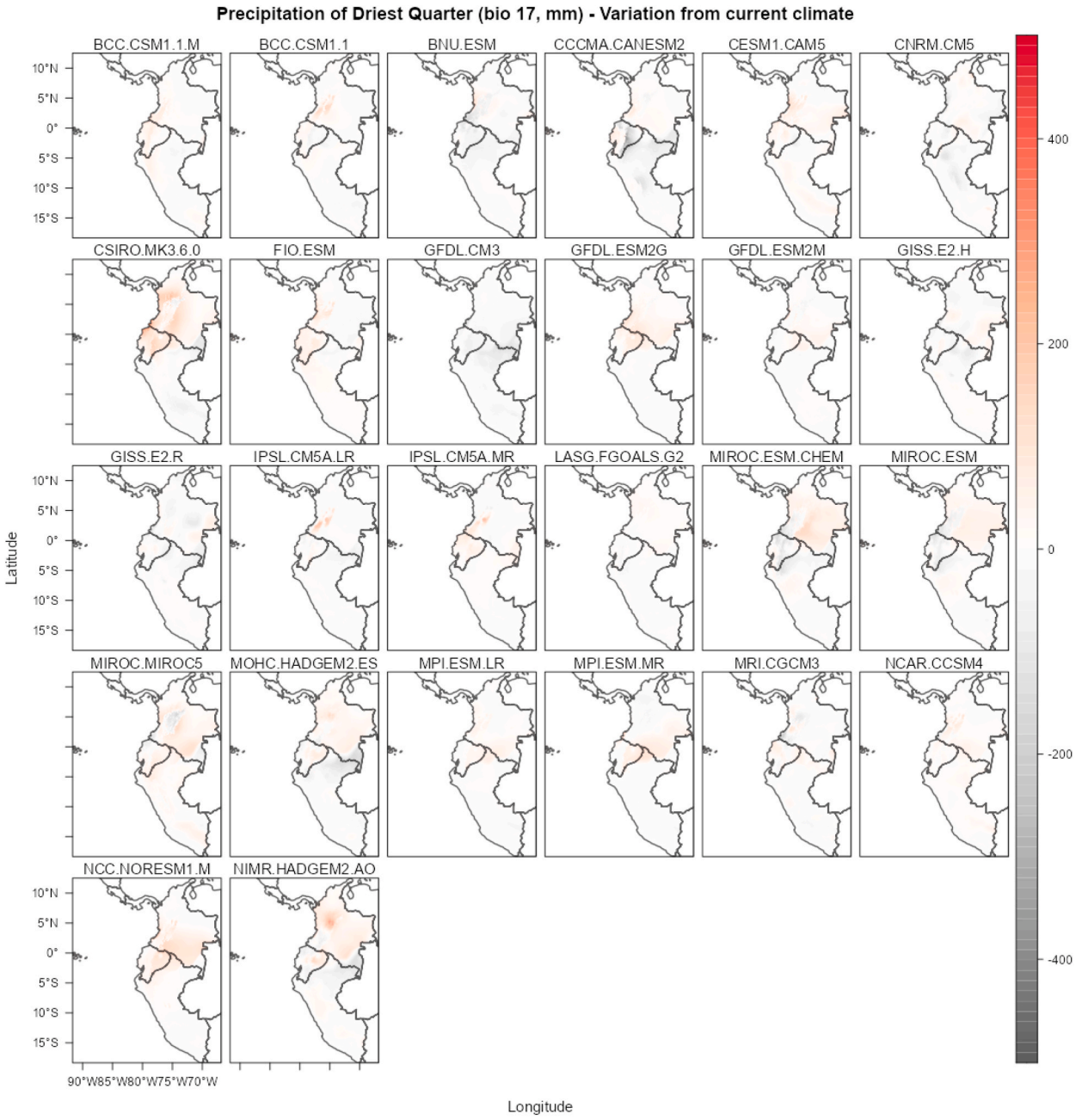

Fig. 9. Differences for the Precipitation of Driest Quarter bio17 (mm) for the RCP 2.6-2050 and the baseline (1970–2000). Where red indicates an increase in temperature, while gray indicates a decrease.

$= 3.7 \times 10^{-24}$) for the Sechura ecoregion that is not following a normal distribution is accepted.

In Fig. S6, the median temperature (°C) obtained for this ecoregion in the baseline period (1970–2000) was 17.22 °C. After that, the medians of temperature (°C) for the RCPs 2050 (2.6, 4.5, and 8.5) were calculated, showing an increase in units; these medians were 18.22 °C, 18.69 °C, and 19.17 °C, respectively. On the other hand, precipitation (mm) medians were calculated for the baseline and the RCPs (2.6, 4.5, and 8.5) for 2050 (Fig. S6). These medians were 64 mm; 56.93 mm; 57.71 mm, and 58.57 mm, respectively. The three RCPs medians for precipitation are lower than the median precipitation for the baseline.

3.5.1.1. Kruskal-Wallis test for temperature (°C) in the Sechura Ecoregion. In Figs. 19 and 20, pairwise comparisons were made for temperature (°C) and precipitation (mm) for the baseline and the three climate change scenarios for 2050 in this ecoregion.

The Kruskal-Wallis test (Table S16) and Fig. 19 showed that there is very strong (or convincing) (*p-value* < 0.001) evidence against

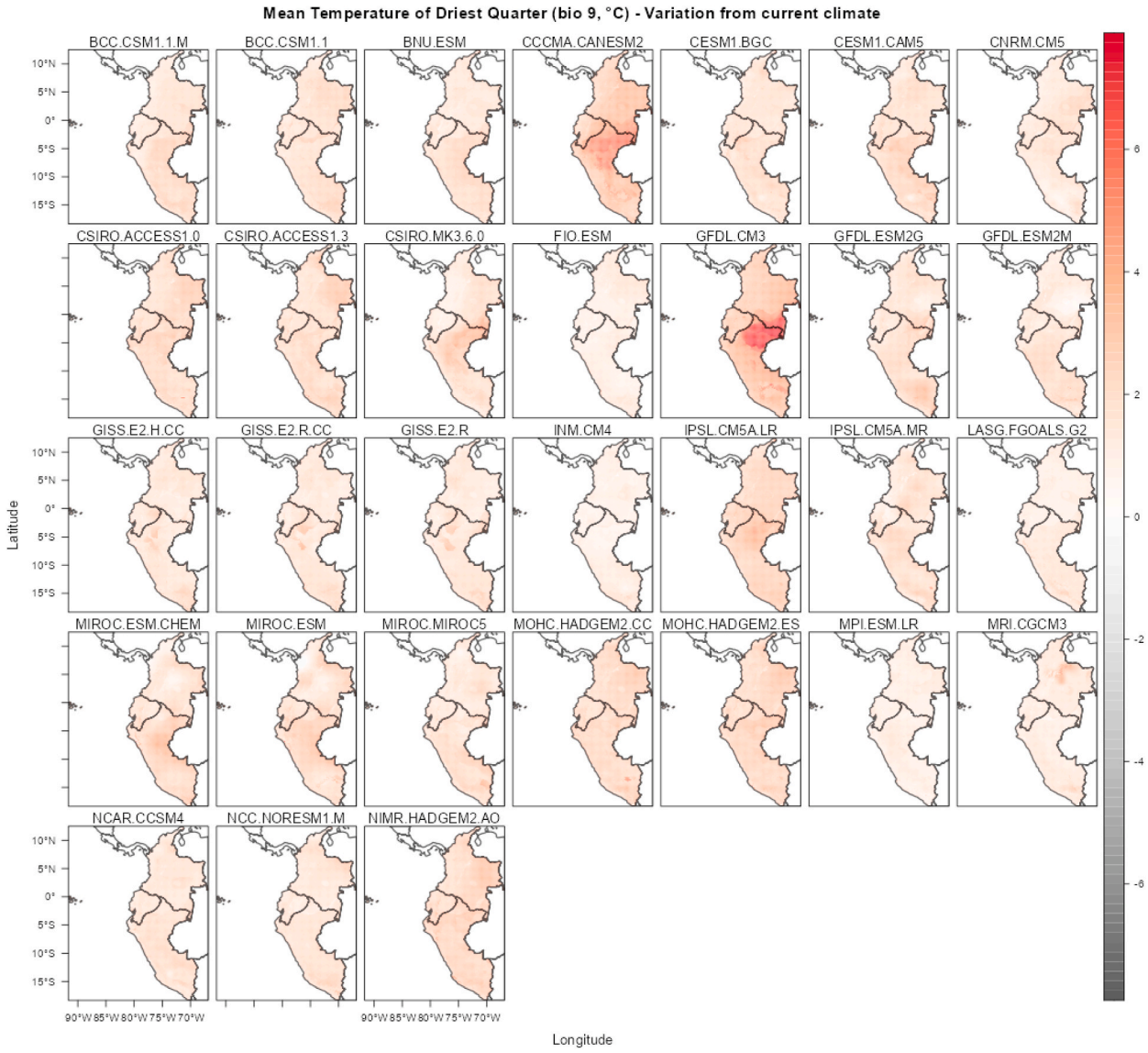

Fig. 10. Differences for the Mean Temperature of Driest Quarter bio9 (°C) for the RCP 4.5-2050 and the baseline (1970–2000). Where red indicates an increase in temperature, while gray indicates a decrease.

the null hypothesis that the median for temperature (C°) between the baseline and the three RCPs 2050 (2.6; 4.5 and 8.5) are equal and in favor that there is at least one pair of differences among the four medians in the Sechura Ecoregion.

That is, we reject H_0: $M_{1970\text{-}2000} = M_{26} = M_{45} = M_{85}$ in favor of H_1: $M_i \neq M_j$ for some $i \neq j$ where i, j represent the temperature (C°) for the baseline and the three RCPs scenarios 1970–2000, 26, 45 and 8.5.

3.5.1.2. Kruskal-Wallis test for precipitation (mm) in the Sechura Ecoregion. The Kruskal-Wallis test and Fig. 20 and Table S17 showed that there is very strong (or convincing) (p-*value* < 0.001) evidence against the null hypothesis that the median for precipitation (mm) between the baseline and the three RCPs 2050 (2.6; 4.5 and 8.5) are equal and in favor that there is at least one pair of differences among the four medians in the Sechura Ecoregion. That is, we reject H_0: $M_{1970\text{-}2000} = M_{26} = M_{45} = M_{85}$ in favor of H_1: $M_i \neq M_j$ for some $i \neq j$ where i, j represent the precipitation (mm) for the baseline and the three RCPs scenarios 1970–2000, 26, 45 and 8.5.

3.5.2. Páramo Ecoregion

The distribution of temperature (°C) and precipitation for 1970–2000 and three climate change scenarios for the Páramo ecoregion respectively are shown in Figs. 21 and 22. In the case of temperature, there is a normal distribution (Fig. 21) for the baseline and the three RCPs, and in the case of precipitation, there is a Skewed Right distribution of the data for the baseline and bimodal distribution for the RCPs 2.6, 4.5 and 8.5 (Fig. 22).

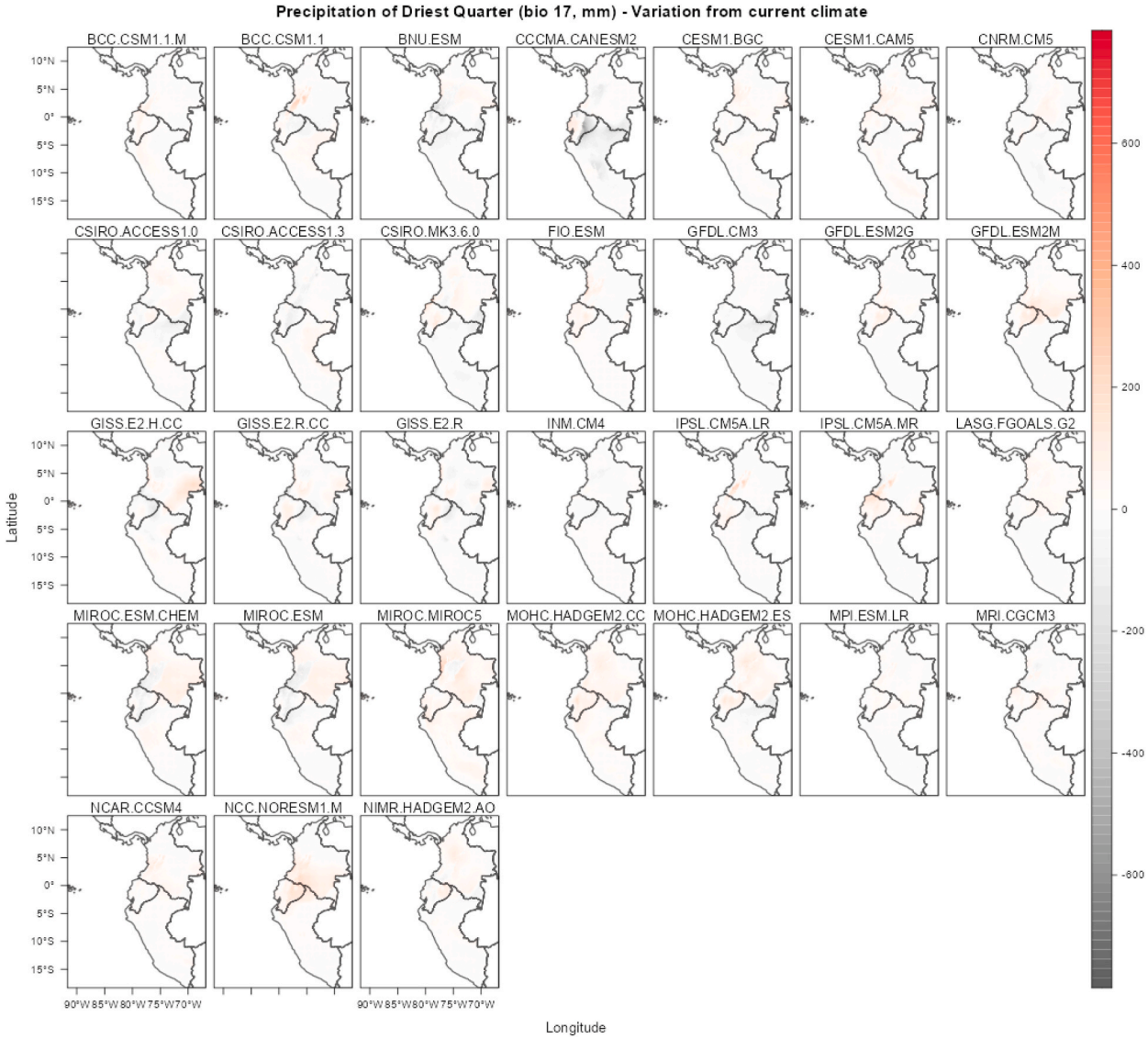

Fig. 11. Differences for the Precipitation of Driest Quarter bio17 (mm) for the RCP 4.5-2050 and the baseline (1970–2000). Where red indicates an increase in temperature, while gray indicates a decrease.

Q-Q plots, histograms, and boxplots for temperature (°C) and precipitation (mm) for the baseline (1970–2000), and the three RCPs 2.6, 4.5, and 8.5 for 2050 in the Páramo ecoregion were analyzed and suggest that there are serious violations of normality assumptions (Skewed) and several atypical values for low and high temperatures (Baseline and RCPs). These atypical values are also observed for annual precipitation, for example, in the baseline, we have these values for both low and high precipitation, and in the RCPs, only for high precipitation (Figs. S7, S8, and S9).

The Anderson-Darling normality test was performed for the temperature (°C) (Table S12) and annual precipitation (mm) (Table S13) for this ecoregion. There is very strong evidence to reject that the data for temperature (*p-value* $= 3.7 \times 10^{-24}$) and annual precipitation (*p-value* $= 3.7 \times 10^{-24}$) follow a normal distribution for the baseline and the three RCPs in 2050. So, the alternative hypothesis is accepted that the temperature and precipitation for the Páramo ecoregion that is not following a normal distribution.

The median temperature (°C) obtained for this ecoregion in the baseline period (1970–2000) was 7.80 °C. After that, the temperature medians (°C) for the RCPs in 2050 (2.6, 4.5, and 8.5) were calculated (Fig. S9), showing an increase in each case. The median values were 9.01 °C, 9.39 °C, and 9.88 °C, respectively. On the other hand, precipitation (mm) medians were calculated for the baseline and the RCPs (2.6, 4.5, and 8.5) for 2050, these medians were 1073.00 mm; 1153.50 mm; 1166.53 mm, and 1176.64 mm respectively (Fig. S9). The three RCPs medians for precipitation are lower than the median precipitation for the baseline.

3.5.2.1. Kruskal-Wallis test for temperature (°C) in the Páramo Ecoregion. In Figs. 23 and 24, pairwise comparisons were made for

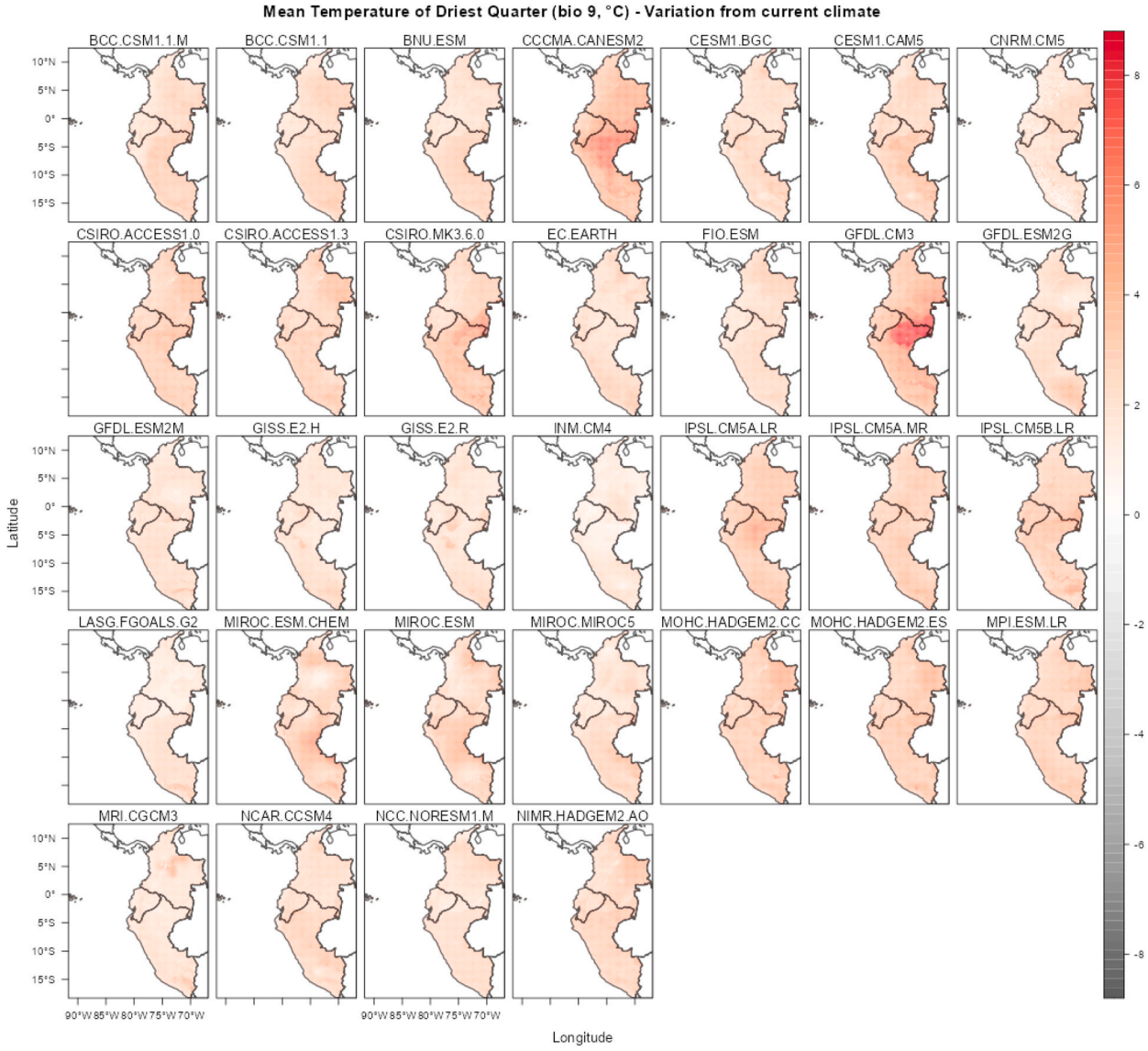

Fig. 12. Differences for the Mean Temperature of Driest Quarter bio9 (°C) for the RCP 8.5-2050 and the baseline (1970–2000). Where red indicates an increase in temperature, while gray indicates a decrease.

temperature (°C) and precipitation (mm) for the baseline and the three climate change scenarios for 2050 in this ecoregion.

The Kruskal-Wallis test and Fig. 23 and Table S18 showed that there is very strong (or convincing) (*p-value* < 0.001) evidence against the null hypothesis that the median for temperature (C°) between the baseline and the three RCPs 2050 (2.6; 4.5 and 8.5) are equal and in favor that there is at least one pair of differences among the four medians in the Páramo Ecoregion.

That is, we reject H_0: $M_{1970\text{-}2000} = M_{26} = M_{45} = M_{85}$ in favor of H_1: $M_i \neq M_j$ for some $i \neq j$ where *i, j* represent the temperature (C°) for the baseline and the three RCPs scenarios 1970–2000, 26, 45 and 8.5.

3.5.2.2. Kruskal-Wallis test for precipitation (mm) in the Páramo Ecoregion. The Kruskal-Wallis test and Fig. 24 and Table S19 showed that there is very strong (or convincing) (*p-value* < 0.001) evidence against the null hypothesis that the median for precipitation (mm) between the baseline and the three RCPs 2050 (2.6; 4.5 and 8.5) are equal and in favor that there is at least one pair of differences among the four medians in the Sechura Ecoregion.

That is, we reject H_0: $M_{1970\text{-}2000} = M_{26} = M_{45} = M_{85}$ in favor of H_1: $M_i \neq M_j$ for some $i \neq j$ where *i, j* represent the precipitation (mm) for the baseline and the three RCPs scenarios 1970–2000, 26, 45 and 8.5.

3.5.3. Napo Ecoregion

The distribution of temperature (°C) and precipitation for 1970–2000 and three climate change scenarios for the Napo ecoregion

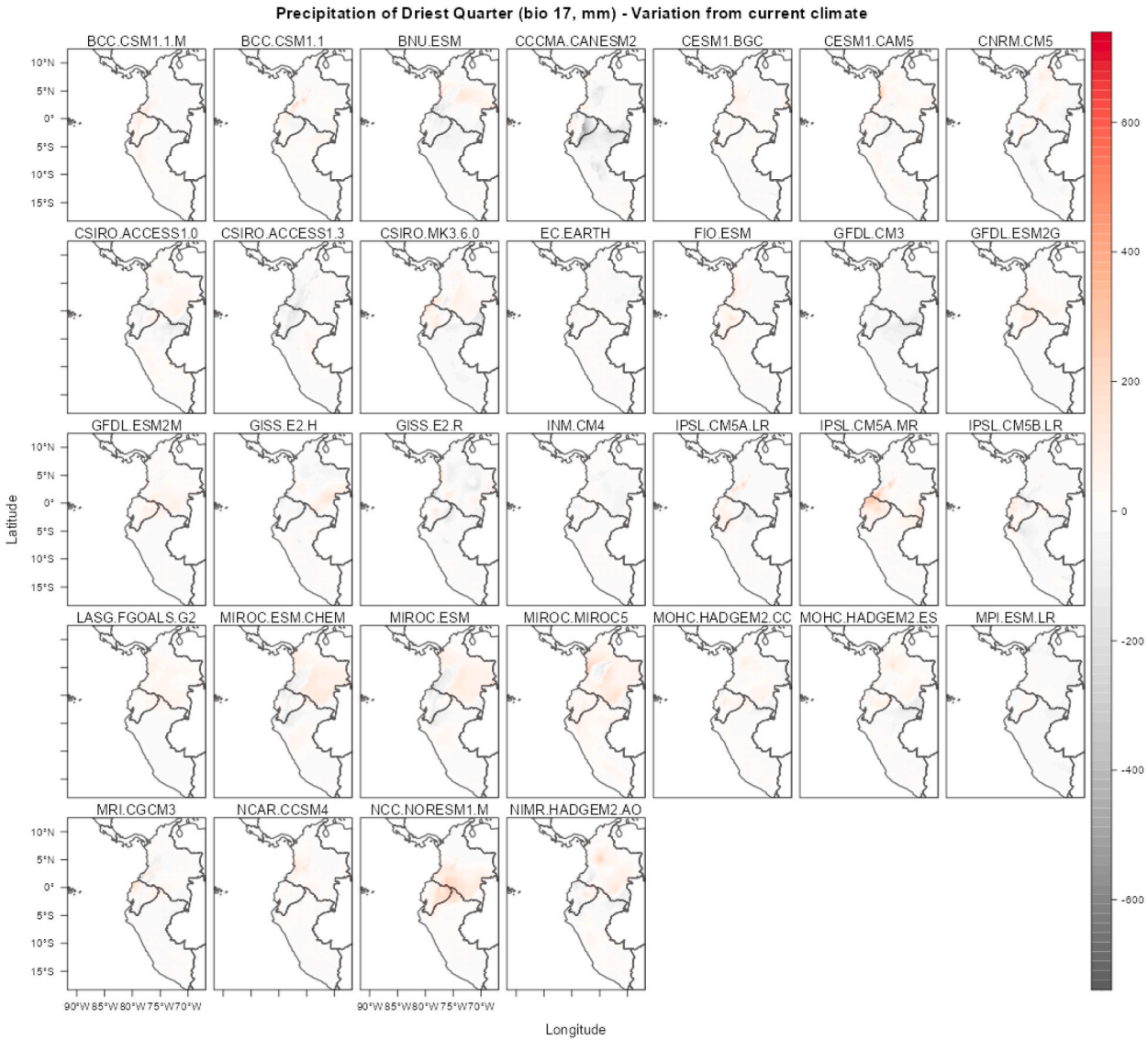

Fig. 13. Differences for the Precipitation of Driest Quarter bio17 (mm) for the RCP 8.5-2050 and the baseline (1970–2000). Where red indicates an increase in temperature, while gray indicates a decrease.

Table 3
Average annual temperature (°C) for the baseline (1970–2000) and 2050 RCP 2.6 (1 km).

Ecoregions	Baseline (1970–2000)						RCP2.6					
	x	Min value	Max value	Std Dev.	CV	M	x	Min value	Max value	Std Dev.	CV	M
Sechura Desert (Deserts & Xeric Shrublands)	15.22	−3.47	23.11	5.36	35.22	2.84	16.35	−3.46	24.93	5.35	32.72	3.06
Páramo (Montane Grasslands & Shrublands)	8	−4.35	24.58	2.68	33.50	2.99	9.24	−4.66	25.79	2.82	30.52	3.28
Napo moist forests (Tropical & Subtropical Moist Broadleaf Forests)	25.64	17.88	27.13	0.75	2.93	34.19	27.23	18.61	28.53	0.73	2.68	37.30

respectively are shown in Figs. 25 and 26. In the case of temperature, there is a Skewed Left distribution (Fig. 25) for the baseline and the three RCPs, and in the case of precipitation, there is a Multimodal distribution of the data for the baseline, and for the RCPs 2.6, 4.5 and 8.5 (Fig. 26).

Table 4
Average annual temperature (°C) for the 2050 RCPs 4.5 and 8.5 (1 km).

Ecoregions	RCP 4.5						RCP 8.5					
	x	Min value	Max value	Std Dev.	CV	M	x	Min value	Max value	Std Dev.	CV	M
Sechura Desert (Deserts & Xeric Shrublands)	16.81	−2.89	25.28	5.32	31.65	3.16	17.3	−2.39	25.66	5.31	30.69	3.26
Páramo (Montane Grasslands & Shrublands)	9.63	−4.25	26.13	2.82	29.28	3.41	10.11	−3.86	26.51	2.84	28.09	3.56
Napo moist forests (Tropical & Subtropical Moist Broadleaf Forests)	27.66	19.04	28.99	0.77	2.78	35.92	28.2	19.53	29.57	0.78	2.77	36.15

Table 5
Annual precipitation (mm) for the baseline (1970–2000) and RCP 2.6 (1 km).

Ecoregions	Baseline (1970–2000)						RCP2.6					
	Annual pp	Min value	Max value	Std Dev.	CV	M	Annual pp	Min value	Max value	Std Dev.	CV	M
Sechura Desert (Deserts & Xeric Shrublands)	183.72	0	1194	225.5	122.74	0.81	207.12	0	1773.36	279.42	134.91	0.74
Páramo (Montane Grasslands & Shrublands)	1151.4	262	3169	329.5	28.62	3.49	1301.34	302.93	3645.21	495.85	38.10	2.62
Napo moist forests (Tropical & Subtropical Moist Broadleaf Forests)	2977.5	1630	4778	493.47	16.57	6.03	2854.4	1840.2	5247.5	471.72	16.53	6.05

Q-Q plots, histograms, and boxplots for temperature and precipitation for the baseline (1970–2000) and the three RCPs 2.6, 4.5, and 8.5 for 2050 in the Sechura ecoregion were analyzed and suggest that there are serious violations of normality assumptions (Skewed) and several atypical values for low temperatures and high precipitation (Figures S10, S11 and S12).

The Anderson-Darling normality test was performed for the temperature (Table S14) and precipitation data (Table S15) for this ecoregion; there is very strong evidence to reject that the data follow a normal distribution for the baseline and the three RCPs in 2050. Therefore, the alternative hypothesis is accepted that temperature ($p\text{-}value = 3.7 \times 10^{-24}$) and precipitation ($p\text{-}value = 3.7 \times 10^{-24}$) for the Napo ecoregion that is not following a normal distribution.

The median temperature (°C) obtained for this ecoregion in the baseline period (1970–2000) was 25.66 °C. After that, the temperature medians (°C) for the RCPs 2050 (2.6, 4.5, and 8.5) were calculated, showing an increase in units; these medians were 27.35 °C, 27.29 °C, and 28.34 °C, respectively (Fig. S12). On the other hand, precipitation (mm) medians were calculated for the baseline and the RCPs (2.6, 4.5, and 8.5) for 2050, these medians were 2972.00 mm; 2823.14 mm; 2901.29 mm, and 2905.21 mm respectively (Fig. S12). The three RCPs medians for precipitation are lower than the median precipitation for the baseline.

3.5.3.1. Kruskal-Wallis test for temperature (°C) in the Napo Ecoregion. In Figs. 27 and 28, pairwise comparisons were made for temperature (°C) and precipitation (mm) for the baseline and the three climate change scenarios for 2050 in this ecoregion.

The Kruskal-Wallis test and Fig. 27 showed that there is very strong (or convincing) ($p\text{-}value < 0.001$) evidence against the null hypothesis that the median for temperature (C°) between the baseline and the three RCPs 2050 (2.6; 4.5 and 8.5) are equal and in favor that there is at least one pair of differences among the four medians in the Napo Ecoregion (Table S20). That is, we reject H_0: $M_{1970\text{-}2000} = M_{26} = M_{45} = M_{85}$ in favor of H_1: $M_i \neq M_j$ for some $i \neq j$ where i, j represent the temperature (C°) for the baseline and the three RCPs scenarios 1970–2000, 26, 45 and 8.5.

3.5.3.2. Kruskal-Wallis test for precipitation (mm) in the Napo Ecoregion. The Kruskal-Wallis test and Fig. 28 and Table S21 showed that there is very strong (or convincing) ($p\text{-}value < 0.001$) evidence against the null hypothesis that the median for precipitation (mm) between the baseline and the three RCPs 2050 (2.6; 4.5 and 8.5) are equal and in favor that there is at least one pair of differences among the four medians in the Napo Ecoregion.

That is, we reject H_0: $M_{1970\text{-}2000} = M_{26} = M_{45} = M_{85}$ in favor of H_1: $M_i \neq M_j$ for some $i \neq j$ where i, j represent the precipitation (mm) for the baseline and the three RCPs scenarios 1970–2000, 26, 45 and 8.5.

Lastly, we have the density plots that indicate where the data are most dense or likely, i.e., these plots allow us to visualize where the average annual temperature and annual precipitation data for the baseline (1970–2000) and the three RCPs for 2050 (2.6, 4.5 and 8.5) are most dense (Figures S13, S14 and S15).

In general, the temperature density curves for the three RCPs in the three ecoregions compared to the baseline are shifted to the right, which means that they show increases in mean annual temperatures, and the low temperatures and high temperatures increase

Table 6
Annual precipitation (mm) for the RCPs 4.5 and 8.5 (1 km).

Ecoregions	RCP 4.5						RCP 8.5					
	Annual pp	Min value	Max value	Std Dev.	CV	M	Annual pp	Min value	Max value	Std Dev.	CV	M
Sechura Desert (Deserts & Xeric Shrublands)	209.95	0	1787.21	283.29	134.93	0.74	214.50	0	1841.86	290.47	135.42	0.74
Páramo (Montane Grasslands & Shrublands)	1307.97	307.50	3635.50	491.39	37.57	2.66	1311.11	319.43	3658.71	484.57	36.96	2.71
Napo moist forests (Tropical & Subtropical Moist Broadleaf Forests)	2938.57	1867.07	5336.86	476.07	16.20	6.17	2940.21	1866	5371.64	479.75	16.32	6.13

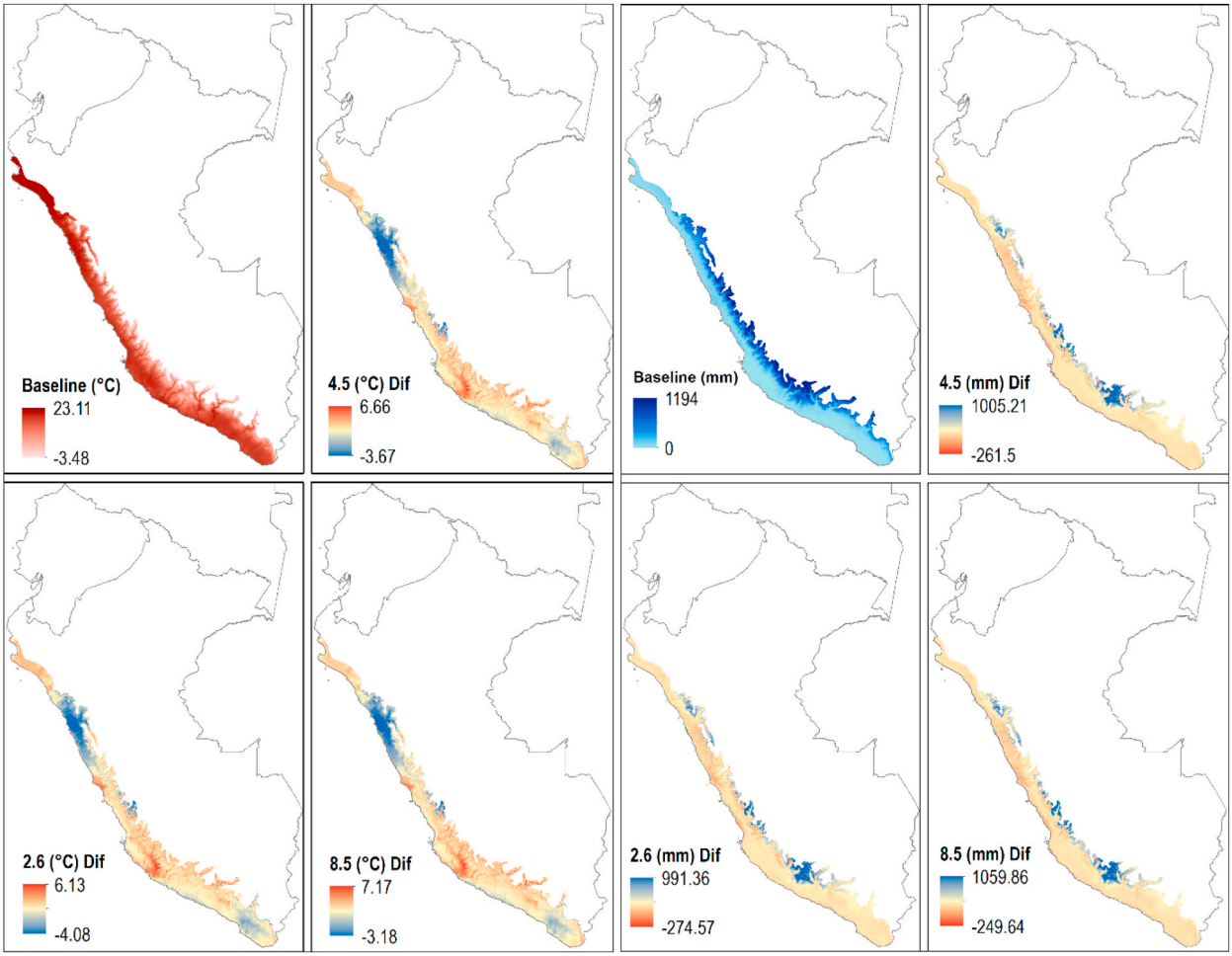

Fig. 14. Differences for temperature (°C) (on the left) and annual precipitation (mm) (on the right) for the RCPs 2.6, 4.5, and 8.5 for 2050 (ensembles from 14 GCMs) vs the baseline (1970–2000) in the Sechura ecoregion (1 km).

their value. On the other hand, in the case of precipitation, there is a slight increase in annual precipitation for high values for the Sechura desert in the three RCPs compared to the baseline (Fig. S13). Also, for the Páramo ecoregion, there is a decrease in density or probability for annual precipitation near or at 1000 mm for RCPs 2.6, 4.5, and 8.5 in 2050 compared to the baseline, but a slight increase in the density or probability of precipitation near or at 2500 mm is observed (Fig. S14). Then, for the Napo ecoregion for the three RCPs in 2050 compared to the baseline, there is a decrease in precipitation density near or at values of 2300 mm and 3200 mm, but there is an increase for precipitation density at values of 2700 mm up to 2900 mm (Fig. S15).

4. Discussion

The analysis of changes in temperature and precipitation for the baseline (1970-200) and for the 2050 RCPs (2.6, 4.5, and 8.5) are important before using SDM models for species or ecoregions in the three countries, as mentioned by Ref. [28].

Analyzing climate change using variables such as temperature (C°) and annual precipitation (mm) in three bordering countries from official data published by their National Meteorological and Hydrological Services is a bit complex. The Andean and Amazonian zones are poorly instrumented, and the number of stations varies greatly from one country to another [25,89,90], making it very difficult to make climate change projections jointly for the three countries. In tropical areas such as Brazil, weather stations help to establish baselines for the analysis of environmental variables such as precipitation. Annual rainfall remained constant (1979–2019), but extreme rainfall events were more concentrated in shorter periods [12].

For regional Climate Change studies, standardized climate data is needed in terms of temporal and spatial resolution (extent, resolution, and Coordinate Reference Systems), for which data from Climate Change, Agriculture, and Food Security ("ccafs") and WorldClim (CMIP5) were used [27,31].

Some evidence considered overwhelming of climate change estimates that global temperature is projected to increase by up to 4 °C by 2100 [1], with alterations in precipitation patterns. However, in our research, some GCMs (10 min resolution) (Tables S3 and S6.),

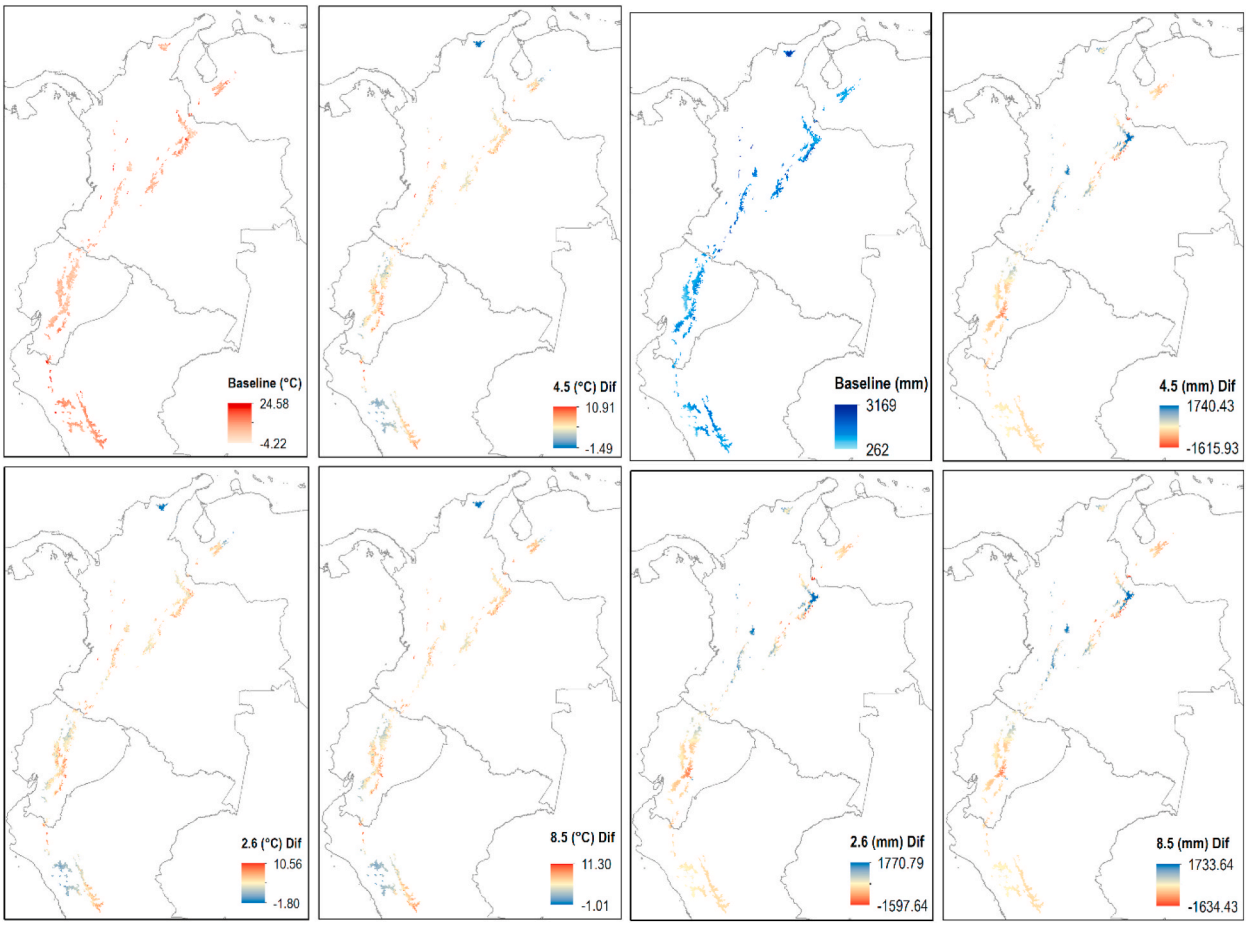

Fig. 15. Differences for temperature (°C) (on the left) and annual precipitation (mm) (on the right) for the RCPs 2.6, 4.5, and 8.5 for 2050 (ensembles from 14 GCMs) vs the baseline (1970–2000) in the Páramo ecoregion (1 km).

such as GFDL.CM3 shows already an increase in the average temperature for Peru, Ecuador, and Colombia above 4 °C for RCPs 4.5 and 8.5 in 2050, and the GCM is named IPSL.CM5A.LR also shows an increase in the average temperature above 4 °C in the NAPO ecoregion for the RCP 8.5-2050. Although our analyses of climate change scenarios extend to 2050, other research showed that temperature warming accelerated in some South American ecoregions during 2010–2019 compared to the long-term average [12].

Also, investigations show a reduction in precipitation under SRES (Special Report on Emissions Scenarios) climate change scenarios in the tropics and an increase in precipitation in the southeastern part of South America [22], but this research provides an analysis at the ecoregion level as well as the spatial distribution of precipitation for a baseline (1970–2000) and for three RCPs in 2050. It is also necessary to further investigate the change in rainfall intensities in scenarios of climate change and to see what effects these have on the changes in the annual precipitation value for each study zone.

Understanding changes in climate variability and extremes is challenged by the interactions between changes in mean and variability [91]. The IPCC presents three assumptions for temperature changes in climate change environments with a normal distribution [92–98]. An increase in the mean leads to new temperature records, but a change in the mean implies no change in variability, and the range between the warmest and coldest temperatures does not change. An increase in variability without a change in the mean implies an increase in the probability of hot and cold extremes, as well as in the absolute value of the extremes, and finally, an increase in the mean and variability is also possible, which affects the probability of hot and cold extremes, with more frequent hot events with more extreme high temperatures and fewer cold events. In contrast, in our research, we have temperature data without normal distribution, but when analyzing the temperature density plots for the baseline and the three RCPs in 2050 for the three ecoregions. A shift to the right is observed for the RCPs, which implies that we will have warmer temperatures concerning the baseline (Figs. S13, S14, and S15).

In the case of annual precipitation, it is more complex to analyze in terms of density plots because in no ecoregion do we have a normal distribution for this variable. In the Páramo Ecoregion (Fig. S14), there is a decrease in annual precipitation close to 1000 mm and an increase in annual precipitation to values close to 2000 and 2300 mm. So, in the case of precipitation, for example, changes in total mean precipitation may be accompanied by other changes such as the frequency of precipitation or the shape of the distribution, including its variability, i.e., more in-depth studies such as Intensity-Duration-Frequency of rainfall in climate change environments should be done [99–101]. Nonetheless, in our research, we at least have minimum, maximum, and average values of annual

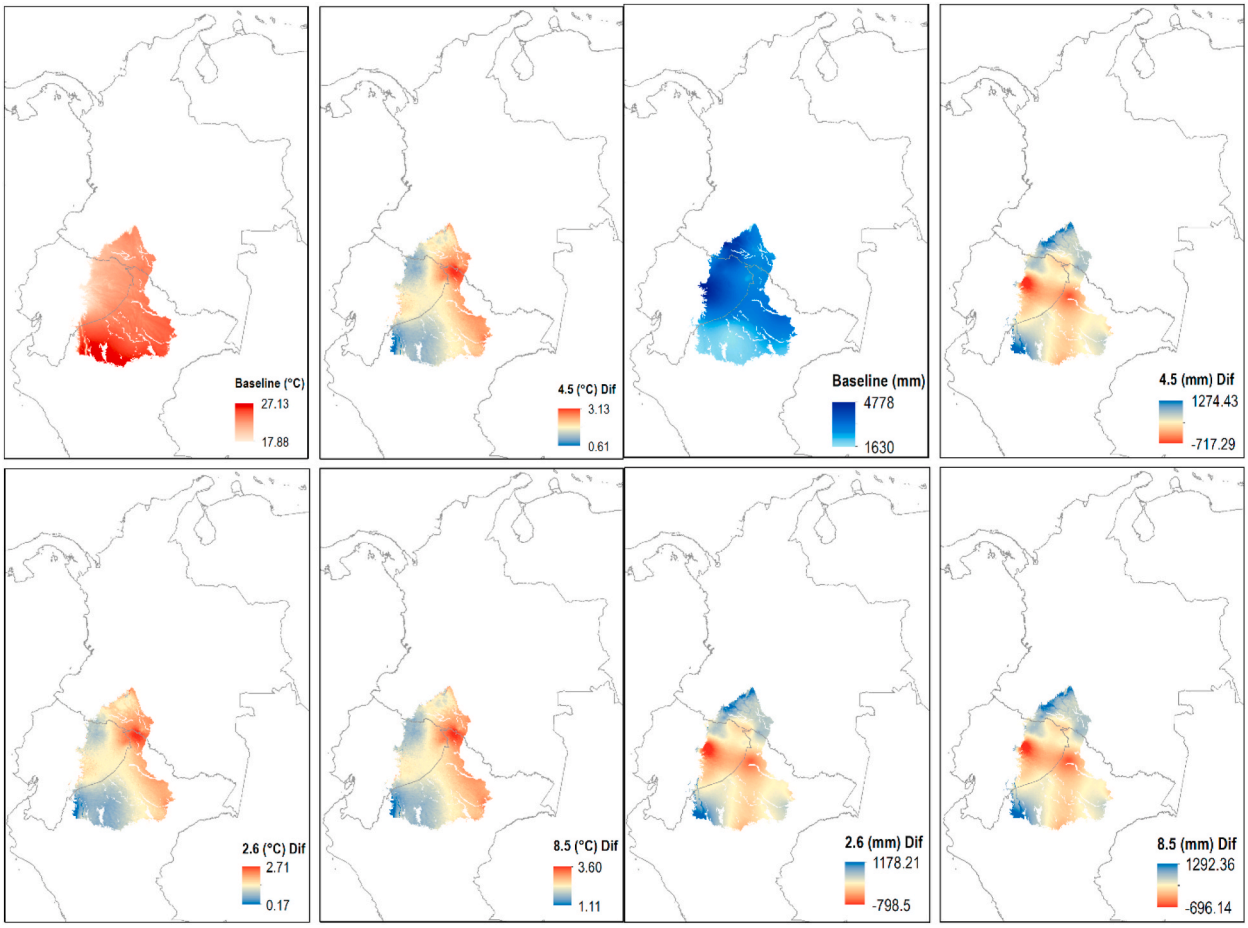

Fig. 16. Differences for temperature (°C) (on the left) and annual precipitation (mm) (on the right) for the RCPs 2.6, 4.5, and 8.5 for 2050 (ensembles from 14 GCMs) vs the baseline (1970–2000) in the Napo ecoregion (1 km).

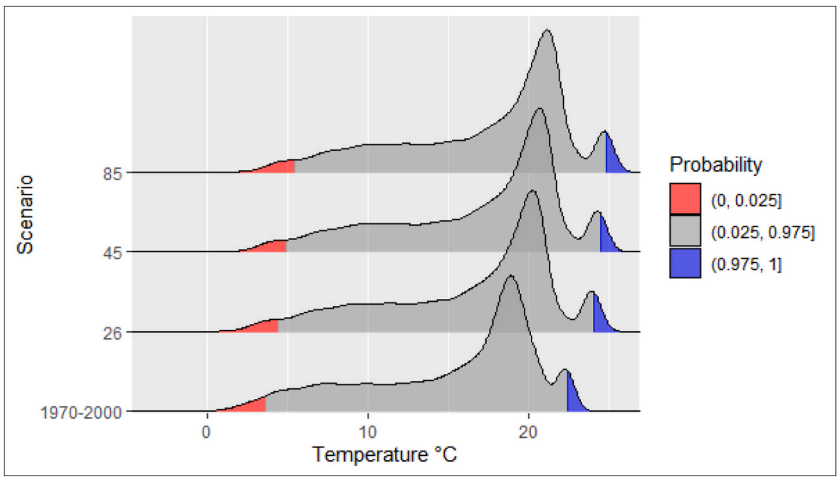

Fig. 17. Distribution of temperature (°C) for 1970–2000 and three climate change scenarios for the Sechura (Desert) ecoregion. The data shows a non-normal distribution, shifting right as global temperature increases in each scenario.

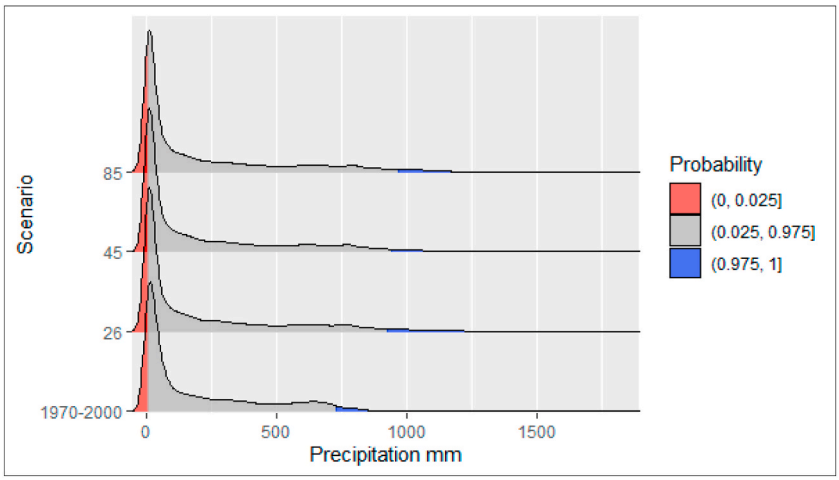

Fig. 18. Distribution of precipitation (mm) for 1970–2000 and three climate change scenarios for the Sechura (Desert) ecoregion. The precipitation data has a non-normal distribution, shifting slightly right as global temperature increases in each scenario.

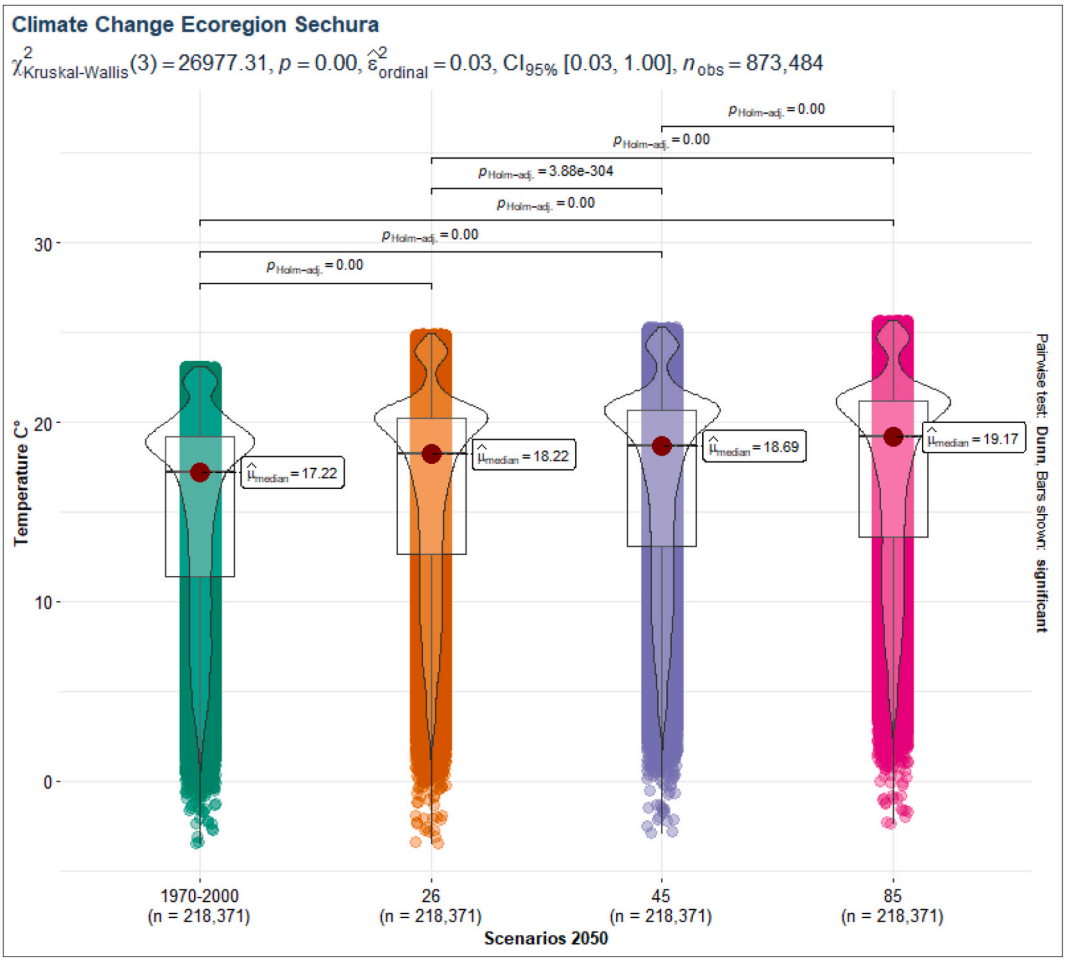

Fig. 19. Comparison of temperature medians (°C) for 1970–2000 and three climate change scenarios for the Sechura (Desert) ecoregion.

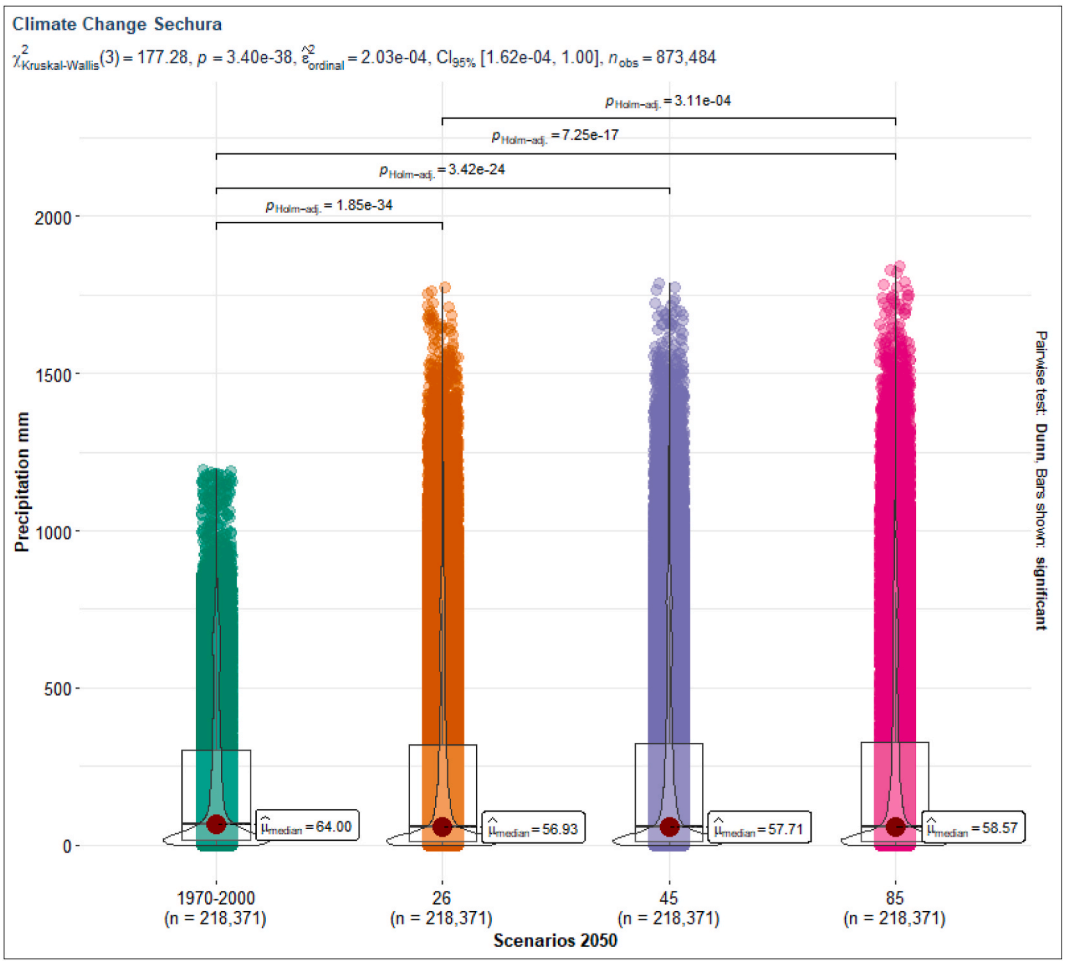

Fig. 20. Comparison of precipitation medians (mm) for 1970–2000 and three climate change scenarios for the Sechura (Desert) ecoregion.

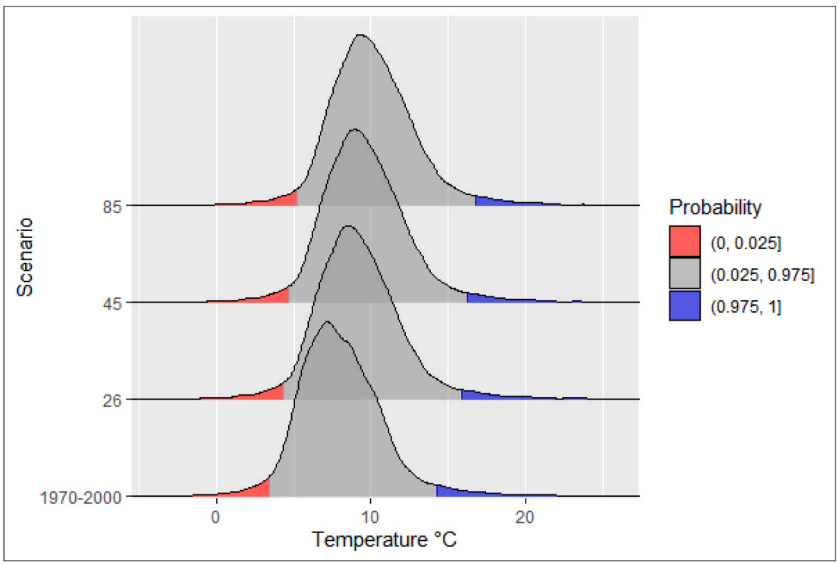

Fig. 21. Distribution of temperature (°C) for 1970–2000 and three climate change scenarios for the Páramo ecoregion. The data shows a non-normal distribution, shifting right as global temperature increases in each scenario.

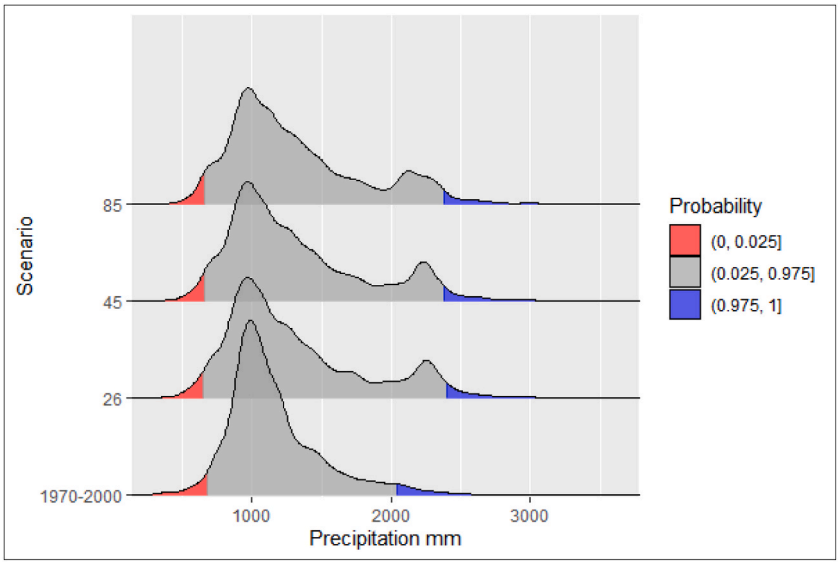

Fig. 22. Distribution of precipitation (mm) for 1970–2000 and three climate change scenarios for the Páramo ecoregion. The precipitation data has a non-normal distribution, shifting slightly right as global temperature increases in each scenario.

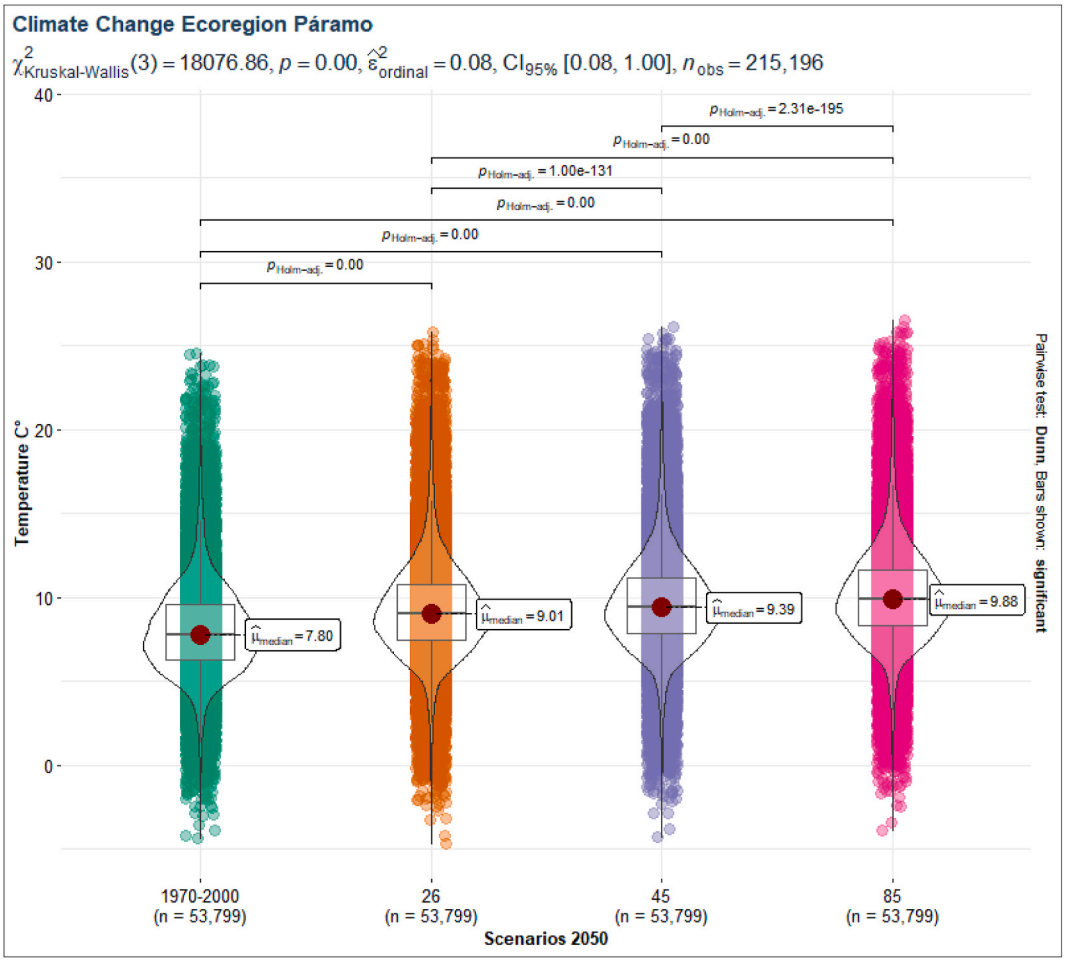

Fig. 23. Comparison of temperature medians (°C) for 1970–2000 and three climate change scenarios for the Páramo ecoregion.

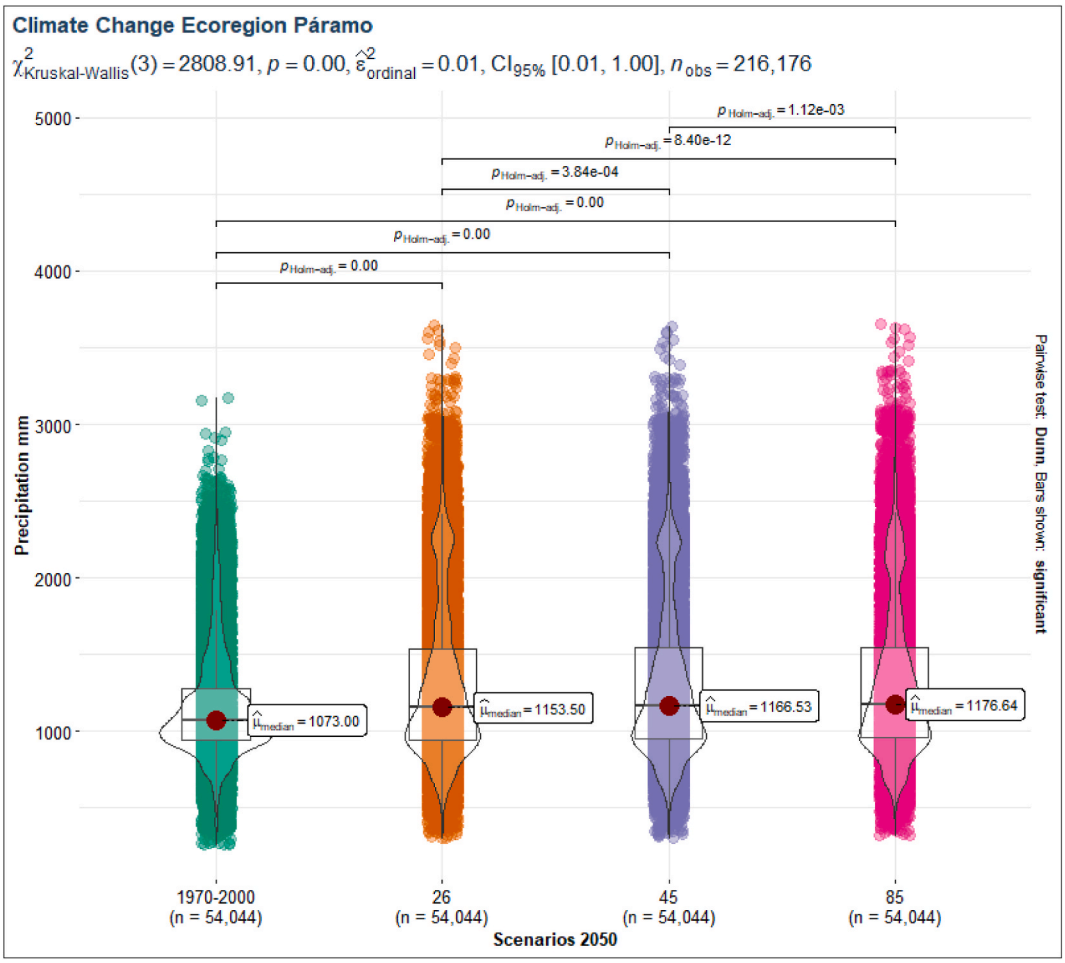

Fig. 24. Comparison of precipitation medians (mm) for 1970–2000 and three climate change scenarios for the Páramo ecoregion.

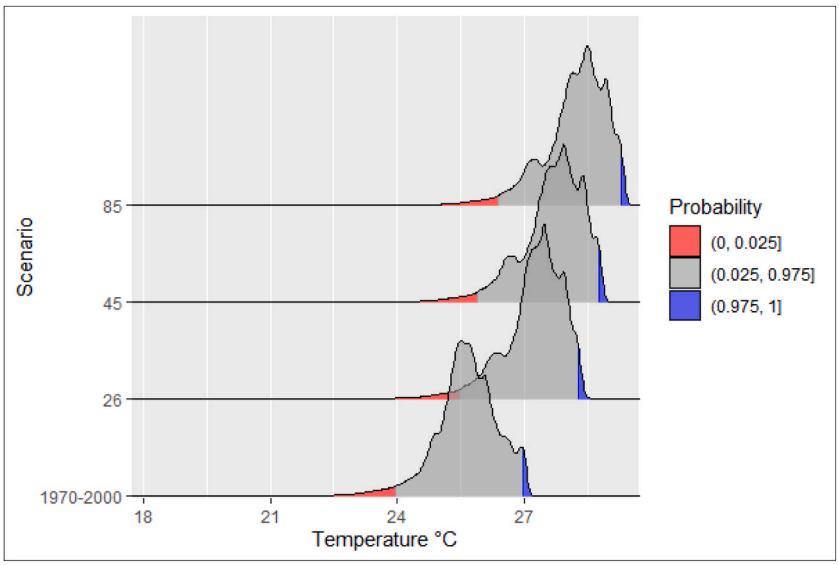

Fig. 25. Distribution of temperature (°C) for 1970–2000 and three climate change scenarios for the Napo ecoregion. The data shows a non-normal distribution, shifting right as global temperature increases in each scenario.

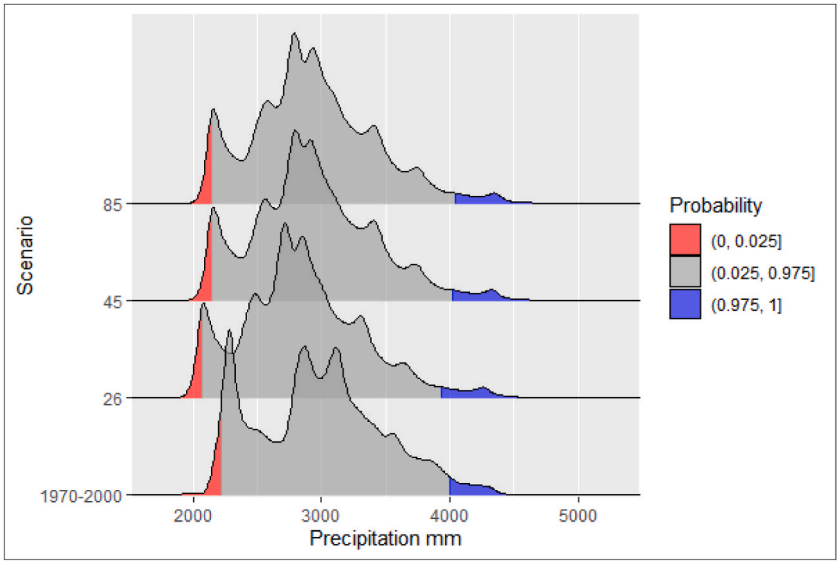

Fig. 26. Distribution of precipitation (mm) for 1970–2000 and three climate change scenarios for the Napo ecoregion. Precipitation data show a non-normal distribution, shifting slightly right and left as global temperature increases in each scenario.

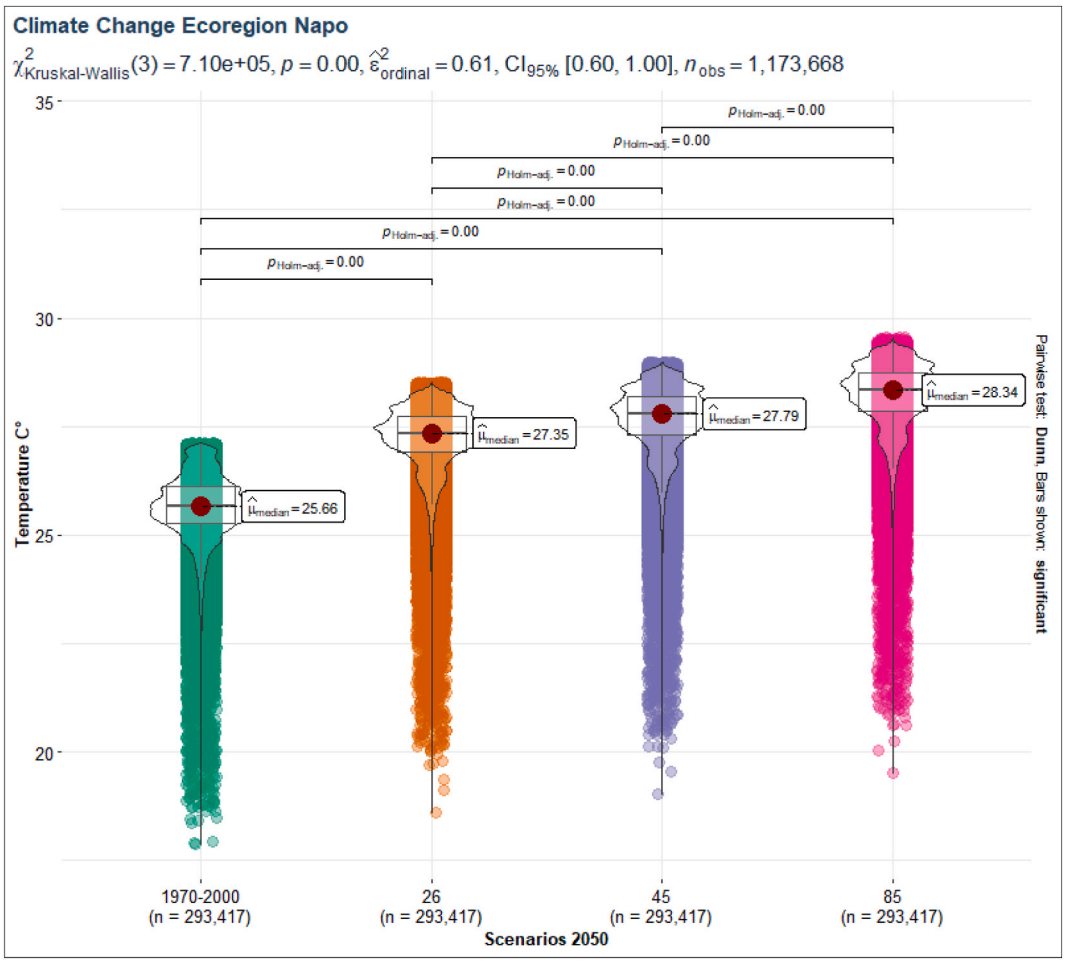

Fig. 27. Comparison of temperature medians (°C) for 1970–2000 and three climate change scenarios for the Napo ecoregion.

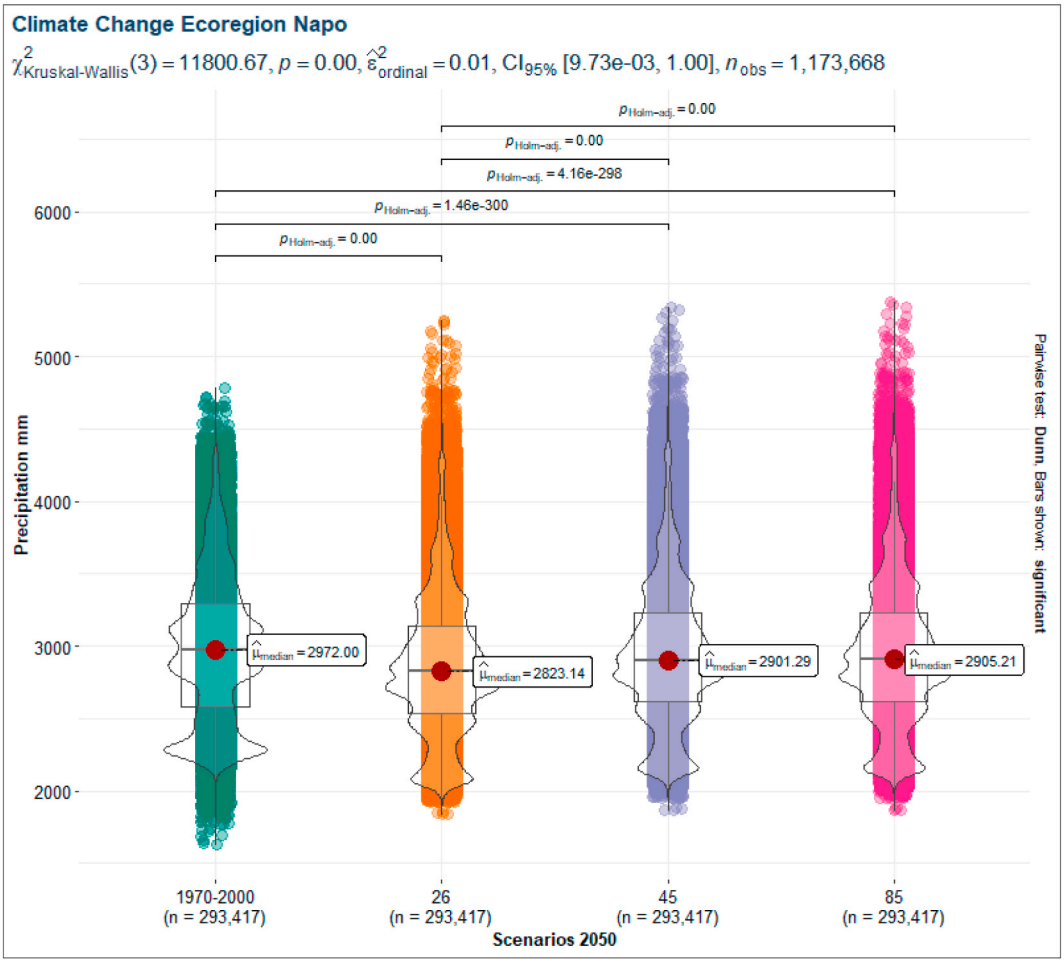

Fig. 28. Comparison of precipitation medians (mm) for 1970–2000 and three climate change scenarios for the Napo ecoregion.

precipitation, which helps us to infer the change in cumulative precipitation for the baseline and the three climate change scenarios at the ecoregion or country level.

Uncertainty in climate modeling refers to the variability and possible inaccuracies in the prediction of future climate conditions, originating from model limitations, emissions scenarios, and internal climate variability, these uncertainties vary according to region, climate variable, and time horizon, analyzing each type can better understand and interpret climate predictions [102].

A technical evaluation of the bias correction method using a "perfect sibling" framework was also carried out, and we showed that it reduces the bias of the climate models by 50–70 % [27]. However, a recommended way to understand the effects of the different GCMs is to use the climate assemblies of these GCMs [103]. This research reviewed published studies and examined spatial changes in temperature and precipitation between the baseline and GCMs for 2050 to better understand these uncertainties in the results, as shown in supplementary tables S1 through S9 to find the differences between the GCMs as well as their differences in values of their estimates, this can help us to analyze GCMs for 2050 with increased temperature and increased precipitation or increased temperature and low precipitation. However, it is suggested to analyze El Niño and La Niña events in South America, as they are increasingly recurrent and could alter temperature and precipitation patterns on an annual basis [12].

Finally, no transformation of the data was performed to achieve a normal distribution for the following reason: the transformation of the data must be done carefully so that the transformed data continues to represent the same physical processes as the original data [8]. Likewise, our research question was to keep the original temperature (°C) and annual precipitation (mm) data for interpretation, both for the baseline and for the climate change scenarios.

5. Conclusions

A general review of changes in temperature (°C) and annual precipitation (mm) at the country and ecoregion level was made, which will help us to understand the variables derived from these, such as Bioclim variables, and to understand the possible effects of these variables on the distribution of species and ecoregions in environments of climate change.

The findings of this study reveal a consistent trend across all General Circulation Models (GCMs) used, indicating a projected rise in annual average temperatures by 2050 at both the country and ecoregion levels. Additionally, a majority of the GCMs suggest an increase in annual precipitation during the same period, but a more local and intensity-duration-frequency (IDF) analysis is needed.

Also, the comparison of medians was important in the statistical analysis part because it allowed us to compare the central tendencies of two or more data sets. The median is a measure of central tendency that represents the average value of a set of data when ordered in ascending or descending order [46,104]. In many cases, the mean is used as a measure of central tendency, however, the extreme values of the data set strongly influence the mean [46]. In contrast, the median is not affected by outliers, making it a more robust measure of central tendency. Comparing medians helped us to establish whether there are significant differences between two or more data sets. In the context of climate change, comparing the median of temperature (°C) or annual precipitation (mm) values over two different periods can help us assess whether a significant change has occurred. Finally, the mean temperature (°C) and the annual precipitation (mm) in the Napo Moist Forest, as represented by the baseline and three Representative Concentration Pathways (RCPs) for 2050, display a relatively large degree of variability compared to the Sechura Desert and Páramo ecoregions. This variability, possibly indicated by a larger range or standard deviation, suggests a more dynamic climatic pattern in the Napo Moist Forest.

CRediT authorship contribution statement

Jaris Veneros: Writing – review & editing, Writing – original draft, Visualization, Validation, Software, Resources, Methodology, Investigation, Funding acquisition, Formal analysis, Data curation, Conceptualization. **Andrew Hansen:** Writing – original draft, Supervision, Resources, Project administration, Methodology, Investigation, Funding acquisition, Formal analysis, Conceptualization. **Patrick Jantz:** Writing – original draft, Supervision, Resources, Project administration, Methodology, Funding acquisition, Formal analysis, Conceptualization. **Dave Roberts:** Writing – original draft, Supervision, Methodology, Formal analysis, Conceptualization. **Elkin Noguera-Urbano:** Writing – review & editing, Writing – original draft, Supervision, Methodology, Investigation, Formal analysis, Conceptualization. **Ligia García:** Writing – review & editing, Writing – original draft, Visualization, Methodology, Investigation, Formal analysis, Conceptualization.

Data and code availability statement

Data will be made available on request. For requesting data, please write to the corresponding author.

Declaration of competing interest

The authors declare that they have no known competing financial interests or personal relationships that could have appeared to influence the work reported in this paper.

Acknowledgments

Acknowledgments To the Universidad Nacional Toribio Rodríguez de Mendoza de Amazonas and the ApiGen Project (CONTRACT No. PE501083491-2023-PROCIENCIA) and the NASA-sponsored Life on Land Project for Montana State University.

Appendix A. Supplementary data

Supplementary data to this article can be found online at https://doi.org/10.1016/j.heliyon.2025.e42459.

References

[1] W. Thuiller, Climate change and the ecologist, Nature 448 (2007), https://doi.org/10.1038/448550a, 7153 2007;448:550–2.
[2] K.J. Willis, S.A. Bhagwat, Biodiversity and climate change, Science 326 (2009) 806–807, https://doi.org/10.1126/science.1178838, 1979.
[3] C. Bellard, C. Bertelsmeier, P. Leadley, W. Thuiller, F. Courchamp, Impacts of climate change on the future of biodiversity, Ecol. Lett. 15 (2012) 365–377, https://doi.org/10.1111/j.1461-0248.2011.01736.x.
[4] P.H. Raven, R.E. Gereau, P.B. Phillipson, C. Chatelain, C.N. Jenkins, C.U. Ulloa, The Distribution of Biodiversity Richness in the Tropics, 2020.
[5] R.C. Gatti, P.B. Reich, J.G.P. Gamarra, T. Crowther, C. Hui, A. Morera, et al., The number of tree species on Earth, Proc. Natl. Acad. Sci. U. S. A. 119 (2022) e2115329119, https://doi.org/10.1073/PNAS.2115329119/SUPPL_FILE/PNAS.2115329119.SAPP.PDF.
[6] M.C. Urban, Accelerating extinction risk from climate change, Science 348 (2015) 571–573, https://doi.org/10.1126/science.aaa4984, 1979.
[7] S.M. Papalexiou, A. Montanari, Global and regional increase of precipitation extremes under global warming, Water Resour. Res. 55 (2019) 4901–4914, https://doi.org/10.1029/2018WR024067.
[8] WMO, Guide to Climatological Practices, 2018.
[9] A. Arguez, R.S. Vose, The definition of the standard WMO climate normal: the key to deriving alternative climate normals, Bull. Am. Meteorol. Soc. 92 (2011) 699–704, https://doi.org/10.1175/2010BAMS2955.1.
[10] P.R. Elsen, E.C. Saxon, B.A. Simmons, M. Ward, B.A. Williams, H.S. Grantham, et al., Accelerated shifts in terrestrial life zones under rapid climate change, Glob. Change Biol. 28 (2022) 918–935, https://doi.org/10.1111/gcb.15962.
[11] V.V. Kharin, F.W. Zwiers, X. Zhang, M. Wehner, Changes in temperature and precipitation extremes in the CMIP5 ensemble, Clim. Change 119 (2013) 345–357, https://doi.org/10.1007/s10584-013-0705-8.

[12] L.O.F. dos Santos, N.G. Machado, M.S. Biudes, H.M.E. Geli, C.A.S. Querino, A.L. Ruhoff, et al., Trends in precipitation and air temperature extremes and their relationship with Sea Surface temperature in the Brazilian Midwest, Atmosphere 14 (2023) 426, https://doi.org/10.3390/ATMOS14030426, 2023;14:426.
[13] E. Ghaderpour, P. Mazzanti, G.S. Mugnozza, F. Bozzano, Coherency and phase delay analyses between land cover and climate across Italy via the least-squares wavelet software, Int. J. Appl. Earth Obs. Geoinf. 118 (2023) 103241, https://doi.org/10.1016/J.JAG.2023.103241.
[14] M. Shawky, M.R. Ahmed, E. Ghaderpour, A. Gupta, G. Achari, A. Dewan, et al., Remote sensing-derived land surface temperature trends over South Asia, Ecol. Inform. 74 (2023) 101969, https://doi.org/10.1016/J.ECOINF.2022.101969.
[15] S. Agrawala, Structural and process history of the intergovernmental Panel on climate change, Clim. Change 39 (1998) 621–642, https://doi.org/10.1023/A:1005312331477.
[16] J. Strandsbjerg Tristan Pedersen, F. Duarte Santos, D. van Vuuren, J. Gupta, R. Encarnação Coelho, B.A. Aparício, et al., An assessment of the performance of scenarios against historical global emissions for IPCC reports, Glob. Environ. Change 66 (2021), https://doi.org/10.1016/j.gloenvcha.2020.102199.
[17] K. Riahi, A. Grübler, N. Nakicenovic, Scenarios of long-term socio-economic and environmental development under climate stabilization, Technol. Forecast. Soc. Change 74 (2007) 887–935, https://doi.org/10.1016/j.techfore.2006.05.026.
[18] D.P. van Vuuren, K. Riahi, K. Calvin, R. Dellink, J. Emmerling, S. Fujimori, et al., The shared socio-economic pathways: trajectories for human development and global environmental change, Glob. Environ. Change 42 (2017) 148–152, https://doi.org/10.1016/j.gloenvcha.2016.10.009.
[19] J.S.T. Pedersen, D.P. van Vuuren, B.A. Aparício, R. Swart, J. Gupta, F.D. Santos, Variability in historical emissions trends suggests a need for a wide range of global scenarios and regional analyses, Commun. Earth Environ. 1 (2020) 1–7, https://doi.org/10.1038/s43247-020-00045-y.
[20] S. Feron, R.R. Cordero, A. Damiani, P.J. Llanillo, J. Jorquera, E. Sepulveda, et al., Observations and projections of heat waves in South America, Sci. Rep. 9 (2019), https://doi.org/10.1038/s41598-019-44614-4.
[21] M.S. Reboita, R.P. Da Rocha, C.G. Dias, R.Y. Ynoue, Climate projections for SouthSouth America: RegCM3 driven by HadCM3 and ECHAM5, Adv. Meteorol. 2014 (2014), https://doi.org/10.1155/2014/376738.
[22] S.C. Chou, A. Lyra, C. Mourão, C. Dereczynski, I. Pilotto, J. Gomes, et al., Assessment of climate change over South America under RCP 4.5 and 8.5 downscaling scenarios, Am. J. Clim. Change (2014) 512–527, https://doi.org/10.4236/ajcc.2014.35043, 03.
[23] C.T. Almeida, J.F. Oliveira-Júnior, R.C. Delgado, P. Cubo, M.C. Ramos, Spatiotemporal rainfall and temperature trends throughout the Brazilian Legal Amazon, 1973–2013, Int. J. Climatol. 37 (2017) 2013–2026, https://doi.org/10.1002/joc.4831.
[24] J. Ospina, C. Domínguez, E. Vega, A. Darghan, L. Rodríguez, Analysis of the water balance under regional scenarios of climate change for arid zones of Colombia, Atmósfera 30 (2017) 63–76, https://doi.org/10.20937/atm.2017.30.01.06.
[25] T. Condom, R. Martínez, J.D. Pabón, F. Costa, L. Pineda, J.J. Nieto, et al., Climatological and hydrological observations for the South American Andes: in situ stations, satellite, and reanalysis data sets, Front. Earth Sci. 8 (2020), https://doi.org/10.3389/feart.2020.00092.
[26] S. Gubler, A. Rossa, G. Avalos, S. Brönnimann, K. Cristobal, M. Croci-Maspoli, et al., Twinning SENAMHI and MeteoSwiss to co-develop climate services for the agricultural sector in Peru, Clim. Serv. 20 (2020), https://doi.org/10.1016/j.cliser.2020.100195.
[27] C. Navarro-Racines, J. Tarapues, P. Thornton, A. Jarvis, J. Ramirez-Villegas, High-resolution and bias-corrected CMIP5 projections for climate change impact assessments, Sci. Data 7 (2020), https://doi.org/10.1038/s41597-019-0343-8.
[28] T.H. Booth, Checking bioclimatic variables that combine temperature and precipitation data before their use in species distribution models, Austral Ecol. 47 (2022) 1506–1514, https://doi.org/10.1111/aec.13234.
[29] J. Fajardo, D. Corcoran, P.R. Roehrdanz, L. Hannah, P.A. Marquet, GCM compareR: a web application to assess differences and assist in the selection of general circulation models for climate change research, Methods Ecol. Evol. 11 (2020) 656–663, https://doi.org/10.1111/2041-210X.13360.
[30] L. Poggio, E. Simonetti, A. Gimona, Enhancing the WorldClim data set for national and regional applications, Sci. Total Environ. 625 (2018) 1628–1643, https://doi.org/10.1016/j.scitotenv.2017.12.258.
[31] S.E. Fick, R.J. Hijmans, WorldClim 2: new 1-km spatial resolution climate surfaces for global land areas, Int. J. Climatol. 37 (2017) 4302–4315, https://doi.org/10.1002/joc.5086.
[32] M.N. Nüez, S.A. Solman, M.F. Cabré, Regional climate change experiments over southern South America. II: climate change scenarios in the late twenty-first century, Clim. Dyn. 32 (2009) 1081–1095, https://doi.org/10.1007/s00382-008-0449-8.
[33] INGEMMET. Geología del Perú, Minero y Metalúrgico - INGEMMET, Instituto Geológico, 1995.
[34] J. Moreno, G. Sevillano, O. Valverde, V. Loayza, R. Haro, J. Zambrano, Soil from the coastal plane. https://doi.org/10.1007/978-3-319-25319-0_2, 2018.
[35] P.L. Bell, Geografía, topografía y clima de Colombia. Manual Comercial e Industrial, 2012, pp. 37–50. Colombia.
[36] D.M. Olson, E. Dinerstein, E.D. Wikramanayake, N.D. Burgess, G.V.N. Powell, E.C. Underwood, et al., Terrestrial ecoregions of the world: a new map of life on earth, Bioscience 51 (2001) 933, https://doi.org/10.1641/0006-3568(2001)051[0933:teotwa]2.0.co;2.
[37] E. Dinerstein, D. Olson, A. Joshi, C. Vynne, N.D. Burgess, E. Wikramanayake, et al., An ecoregion-based approach to protecting half the terrestrial realm, Bioscience 67 (2017) 534–545, https://doi.org/10.1093/biosci/bix014.
[38] M. Block, M. Richter, Impacts of heavy rainfalls in El Nino 1997/98 on the vegetation of Sechura Desert in Northern Peru (A preliminary report), Phytocoenologia 30 (2000) 491–517, https://doi.org/10.1127/phyto/30/2000/491.
[39] Schipper J., Sechura Desert, One Earth, 2017, https://www.oneearth.org/ecoregions/sechura-desert/ (Accessed 20 February 2023).
[40] T. Fuentes-Castillo, H.J. Hernández, P. Pliscoff, Hotspots and ecoregion vulnerability driven by climate change velocity in Southern South America, Reg. Environ. Change 20 (2020), https://doi.org/10.1007/s10113-020-01595-9.
[41] P.C. Guerrero, M. Rosas, M.T.K. Arroyo, J.J. Wiens, Evolutionary lag times and recent origin of the biota of an ancient desert (Atacama-Sechura), Proc. Natl. Acad. Sci. U. S. A. 110 (2013) 11469–11474, https://doi.org/10.1073/pnas.1308721110.
[42] Schipper J., Northern Andean Páramo, One Earth, 2017, https://www.oneearth.org/ecoregions/northern-andean-paramo/ (Accessed 23 February 2023).
[43] Schipper J., Napo Moist Forests, 2017, https://www.oneearth.org/ecoregions/napo-moist-forests/ (Accessed 14 March 2023).
[44] L. García, J. Veneros, S. Chávez, M. Oliva, N. Briceño, Historical world mapping and current distribution in Peru of Cinchona spp.: contribution to restoration and conservation strategies, Figshare (2021) 126290, https://doi.org/10.1016/j.jnc.2022.126290. Dataset.
[45] M.C. Thrun, T. Gehlert, A. Ultsch, Analyzing the fine structure of distributions, PLoS One 15 (2020) 1–20, https://doi.org/10.1371/journal.pone.0238835.
[46] F. Ramsey, D. Schafer, The Statistical Sleuth: a Course in Methods of Data Analysis, 2013.
[47] Gross J., Ligges U., Package 'nortest', Version 1.0-4, Tests for Normality, CRAN (2022). https://cran.r-project.org/web/packages/nortest/. (Accessed 13 October 2022).
[48] M. Horst A, A. Presmanes Hill, K. B. Gorman, Palmer archipelago penguins data in the palmerpenguins R Package - an alternative to Anderson's Irises, R J 14 (2022) 244–254, https://doi.org/10.32614/rj-2022-020.
[49] A. Horst, A. Hill, K. Gorman, Package 'palmerpenguins', Version 0.1.1, Palmer Archipelago (Antarctica) Penguin Data, CRAN (2022). https://allisonhorst.github.io/palmerpenguins/. (Accessed 12 August 2022).
[50] J.W. Gooch, Kruskal-Wallis test, in: Encyclopedic Dictionary of Polymers, 2011, pp. 984–985, https://doi.org/10.1007/978-1-4419-6247-8_15268.
[51] S. Siegel, Nonparametric statistics, Am. Statistician 11 (1957) 13–19, https://doi.org/10.1080/00031305.1957.10501091.
[52] J.S.M. Coleman, Atmospheric Science: Meteorology and Climatology 1450 (2015) 1–7, https://doi.org/10.1016/B978-0-12-409548-9.09492-6.
[53] M.S. Reboita, C.A.C. Kuki, V.H. Marrafon, C.A. de Souza, G.W.S. Ferreira, T. Teodoro, et al., South America climate change revealed through climate indices projected by GCMs and Eta-RCM ensembles, Clim. Dyn. 58 (2022) 459–485, https://doi.org/10.1007/s00382-021-05918-2.
[54] M. Lazaridis, First Principles of Meteorology, 2011, pp. 67–118, https://doi.org/10.1007/978-94-007-0162-5_2.
[55] M. Hulme, Climates Multiple: Three Baselines, Two Tolerances, One Normal, Academia Letters, 2020, https://doi.org/10.20935/AL102.
[56] L.M. Boschman, Andean mountain building since the Late Cretaceous: a paleoelevation reconstruction, Earth Sci. Rev. 220 (2021) 103640, https://doi.org/10.1016/J.EARSCIREV.2021.103640.
[57] J.C. Espinoza, R. Garreaud, G. Poveda, P.A. Arias, J. Molina-Carpio, M. Masiokas, et al., Hydroclimate of the Andes Part I: main climatic features, Front. Earth Sci. 8 (2020) 1–20, https://doi.org/10.3389/feart.2020.00064.

[58] W.P. Schellart, A geodynamic model of Andean mountain building, Geophys. Res. Abstr. 19 (2017) 2017–7064.
[59] P.W. Rundel, M.O. Dillon, B. Palma, H.A. Mooney, S.L. Gulmon, J.R. Ehleringer, The phytogeography and ecology of the coastal Atacama and Peruvian Deserts, Aliso 13 (1991) 1–49, https://doi.org/10.5642/aliso.19911301.02.
[60] N.C. Pepin, E. Arnone, A. Gobiet, K. Haslinger, S. Kotlarski, C. Notarnicola, E. Palazzi, P. Seibert, S. Serafin, W. Schöner, S. Terzago, J.M. Thornton, M. Vuille, C. Adler, Climate Changes and Their Elevational Patterns in the Mountains of the World, Geophys. Res. Lett. 49 (2022) 1–13, https://doi.org/10.1029/2020RG000730.
[61] J.P. Sierra, P.A. Arias, A.M. Durán-Quesada, K.A. Tapias, S.C. Vieira, J.A. Martínez, The Choco low-level jet: past, present and future, Clim. Dyn. 56 (2021) 2667–2692, https://doi.org/10.1007/s00382-020-05611-w.
[62] J. Yepes, G. Poveda, J.F. Mejía, L. Moreno, C. Rueda, Choco-jex: a research experiment focused on the Chocó low-level jet over the far eastern Pacific and western Colombia, Bull. Am. Meteorol. Soc. 100 (2019) 779–796, https://doi.org/10.1175/BAMS-D-18-0045.1.
[63] N. Nakicenovic, R. Swart (Eds.), Special Report on Emissions Scenarios, Cambridge University Press, Cambridge, 2000.
[64] P. Sands, P. Galizzi (Eds.), United Nations Framework Convention on Climate Change, 9 May 1992, in: Documents in International Environmental Law, Cambridge University Press, Cambridge, 2004, pp. 128-152, doi:10.1017/CBO9781139171380.012.
[65] WMO, State of the Global Climate 2021, WMO-No. 1290, WMO, Geneva, 2022.WMO, FAQs - climate. 2022.
[66] F. Stuart Chapin, P.A. Matson, P.M. Vitousek, Principles of terrestrial ecosystem ecology, Principles of Terrestrial Ecosystem Ecology 1–529 (2012), https://doi.org/10.1007/978-1-4419-9504-9/COVER.
[67] Q. He, B.R. Silliman, Climate change, human impacts, and coastal ecosystems in the Anthropocene, Curr. Biol. 29 (2019) R1021–R1035, https://doi.org/10.1016/J.CUB.2019.08.042.
[68] IPCC, Summary for Policymakers, in: Climate Change 2014: Mitigation of Climate Change, O. Edenhofer, R. Pichs-Madruga, Y. Sokona, E. Farahani, S. Kadner, K. Seyboth, A. Adler, I. Baum, S. Brunner, P. Eickemeier, B. Kriemann, J. Savolainen, S. Schlömer, C. von Stechow, T. Zwickel, J.C. Minx (Eds.), Cambridge University Press, Cambridge, 2014.
[69] M.J. Salinger, Climate variability and change: past, present and future - an overview, Increasing Climate Variability and Change: Reducing the Vulnerability of Agriculture and Forestry (2005) 9–29, https://doi.org/10.1007/1-4020-4166-7_3/COVER.
[70] J.E. Livingston, E. Lövbrand, J. Alkan Olsson, From climates multiple to climate singular: maintaining policy-relevance in the IPCC synthesis report, Environ. Sci. Pol. 90 (2018) 83–90, https://doi.org/10.1016/j.envsci.2018.10.003.
[71] IPCC, Glossary of terms. Glossary of terms, in: Managing the Risks of Extreme Events and Disasters to Advance Climate Change Adaptation, 2012, pp. 555–564, https://doi.org/10.1002/9783527612024.oth1.
[72] IPCC, Emissions scenarios. https://archive.ipcc.ch/ipccreports/sres/emission/index.php?idp=27, 2021. (Accessed 12 September 2021).
[73] J.T.S. Pedersen, D. van Vuuren, J. Gupta, F.D. Santos, J. Edmonds, R. Swart, IPCC emission scenarios: how did critiques affect their quality and relevance 1990–2022? Glob. Environ. Change 75 (2022) 102538 https://doi.org/10.1016/J.GLOENVCHA.2022.102538.
[74] D.P. van Vuuren, J. Edmonds, M. Kainuma, K. Riahi, A. Thomson, K. Hibbard, et al., The representative concentration pathways: an overview, Clim. Change 109 (2011) 5–31, https://doi.org/10.1007/S10584-011-0148-Z/TABLES/4.
[75] H. Carlsen, R.J.T. Klein, P. Wikman-Svahn, Transparent scenario development, Nat. Clim. Change 7 (2017) 613, https://doi.org/10.1038/nclimate3379.
[76] K. Riahi, D.P. van Vuuren, E. Kriegler, J. Edmonds, B.C. O'Neill, S. Fujimori, et al., The Shared Socioeconomic Pathways and their energy, land use, and greenhouse gas emissions implications: an overview, Glob. Environ. Change 42 (2017) 153–168, https://doi.org/10.1016/j.gloenvcha.2016.05.009.
[77] S.C. Stark, D.D. Breshears, S. Aragón, J.C. Villegas, D.J. Law, M.N. Smith, et al., Reframing tropical savannization: linking changes in canopy structure to energy balance alterations that impact climate, Ecosphere 11 (2020), https://doi.org/10.1002/ecs2.3231.
[78] A. Lyra, C. Chou, G. Sampaio, Sensitivity of the Amazon biome to high resolution climate change projections, Acta Amazon 46 (2016) 175–188, https://doi.org/10.1590/1809-4392201502225.
[79] J.P.R. Fernandez, S.H. Franchito, V.B. Rao, Future changes in the aridity of South America from regional climate model projections, Pure Appl. Geophys. 176 (2019) 2719–2728, https://doi.org/10.1007/s00024-019-02108-4.
[80] A. Staal, O.A. Tuinenburg, J.H.C. Bosmans, M. Holmgren, E.H. Van Nes, M. Scheffer, et al., Forest-rainfall cascades buffer against drought across the Amazon, Nat. Clim. Change 8 (2018) 539–543, https://doi.org/10.1038/s41558-018-0177-y.
[81] J. Zevallos, W. Lavado-Casimiro, Climate change impact on Peruvian biomes, Forests 13 (2022), https://doi.org/10.3390/f13020238.
[82] R.R. Torres, R.B. Benassi, F.B. Martins, D.M. Lapola, Projected impacts of 1.5 and 2°C global warming on temperature and precipitation patterns in South America, Int. J. Climatol. 42 (2022) 1597–1611, https://doi.org/10.1002/joc.7322.
[83] C. Tovar, C.A. Arnillas, F. Cuesta, W. Buytaert, Diverging responses of tropical Andean biomes under future climate conditions, PLoS One 8 (2013), https://doi.org/10.1371/journal.pone.0063634.
[84] C. Josse, F. Cuesta, G. Navarro, V. Barrena, E. Cabrera, E. Chacón-Moreno, et al., Ecosistemas de los Andes del Norte y Centro, Comunidad Andina de Naciones, 2009.
[85] R.G.M. Hofstede, L.D. Llambí, Plant diversity in Páramo-Neotropical high mountain humid grasslands, Encyclopedia of the World's Biomes 1–5 (2020) 362–372, https://doi.org/10.1016/B978-0-12-409548-9.11858-5.
[86] R.J. Morris, Anthropogenic impacts on tropical forest biodiversity: a network structure and ecosystem functioning perspective, Phil. Trans. Biol. Sci. 365 (2010) 3709, https://doi.org/10.1098/RSTB.2010.0273.
[87] B.F. Alves de Oliveira, M.J. Bottino, P. Nobre, C.A. Nobre, Deforestation and climate change are projected to increase heat stress risk in the Brazilian Amazon, Commun. Earth Environ. 2 (2021), https://doi.org/10.1038/s43247-021-00275-8.
[88] L.M. Beltrán-Tolosa, C. Navarro-Racines, P. Pradhan, G.S. Cruz-Garcia, R. Solis, M. Quintero, Action needed for staple crops in the Andean-Amazon foothills because of climate change, Mitig. Adapt. Strategies Glob. Change 25 (2020) 1103–1127, https://doi.org/10.1007/s11027-020-09923-4.
[89] L. Campozano, D. Ballari, M. Montenegro, A. Avilés, Future meteorological droughts in Ecuador: decreasing trends and associated spatio-temporal features derived from CMIP5 models, Front. Earth Sci. 8 (2020), https://doi.org/10.3389/feart.2020.00017.
[90] F.L. Newell, I.J. Ausprey, S.K. Robinson, Spatiotemporal climate variability in the Andes of northern Peru: evaluation of gridded datasets to describe cloud forest microclimate and local rainfall, Int. J. Climatol. 42 (2022) 5892–5915, https://doi.org/10.1002/joc.7567.
[91] G.A. Meehl, T. Karl, D.R. Easterling, S. Changnon, R. Pielke, D. Changnon, et al., An introduction to trends in extreme weather and climate events: observations, socioeconomic impacts, terrestrial ecological impacts, and model projections, Bull. Am. Meteorol. Soc. 81 (2000) 413–416, https://doi.org/10.1175/1520-0477(2000)081<0413:aittie>2.3.co;2.
[92] J. Haywood, M. Schulz, Causes of the reduction in uncertainty in the anthropogenic radiative forcing of climate between IPCC (2001) and IPCC (2007), Geophys. Res. Lett. 34 (2007), https://doi.org/10.1029/2007GL030749.
[93] D. Easterling, M. Rusticucci, V. Semenov, L.V. Alexander, S. Allen, G. Benito, et al., Changes in Climate Extremes and Their Impacts on the Natural Physical Environment, 2012, pp. 109–230.
[94] S.C. Lewis, A.D. King, Evolution of mean, variance and extremes in 21st century temperatures, Weather Clim. Extrem. 15 (2017) 1–10, https://doi.org/10.1016/j.wace.2016.11.002.
[95] P.K. Thornton, P.J. Ericksen, M. Herrero, A.J. Challinor, Climate variability and vulnerability to climate change: a review, Glob. Change Biol. 20 (2014) 3313–3328, https://doi.org/10.1111/gcb.12581.
[96] C.K. Folland, T.R. Karl, M. Jim Salinger, Observed climate variability and change, Weather 57 (2002) 269–278, https://doi.org/10.1256/004316502320517353.
[97] E. Kodra, A.R. Ganguly, Asymmetry of projected increases in extreme temperature distributions, Sci. Rep. 4 (2014), https://doi.org/10.1038/srep05884.
[98] J.R. Olsen, Adapting infrastructure and civil engineering practice to a changing climate. https://doi.org/10.1061/9780784479193, 2015.

[99] S. Das, M. Kamruzzaman, A.R.M.T. Islam, Assessment of characteristic changes of regional estimation of extreme rainfall under climate change: a case study in a tropical monsoon region with the climate projections from CMIP6 model, J. Hydrol. (Amst.) 610 (2022) 128002, https://doi.org/10.1016/j.jhydrol.2022.128002.
[100] A.G. Pendergrass, D.L. Hartmann, Changes in the distribution of rain frequency and intensity in response to global warming, J. Clim. 27 (2014) 8372–8383, https://doi.org/10.1175/JCLI-D-14-00183.1.
[101] Y. Sun, D. Wendi, D.E. Kim, S.Y. Liong, Deriving intensity–duration–frequency (IDF) curves using downscaled in situ rainfall assimilated with remote sensing data, Geosci. Lett. 6 (2019), https://doi.org/10.1186/s40562-019-0147-x.
[102] D. Sauchyn, B. Jon, A. Muhammad Rehan, B. Soumik, S. Sheena, Understanding and Accommodating Uncertainty in Climate Change Data: A Primer climatewest.ca Plain Language Version Prepared by the Prairie Adaptation Research Collaborative for ClimateWest, 2022.
[103] A. Ribes, S. Qasmi, N.P. Gillett, Making Climate Projections Conditional on Historical Observations, vol. 7, 2021.
[104] S. Prasad, Measures of central tendencies. Elementary Statistical Methods, 2022, pp. 37–96, https://doi.org/10.1007/978-981-19-0596-4_2.